University of Texas at El Paso
DigitalCommons@UTEP

Open Access Theses & Dissertations

2013-01-01

Endocrine Disrupting Compound 4-Nonylphenol and Neurodegeneration

Jessica Martinez Jurado
University of Texas at El Paso, jmartinez31@miners.utep.edu

Follow this and additional works at: https://digitalcommons.utep.edu/open_etd

 Part of the Biology Commons, and the Environmental Sciences Commons

Recommended Citation
Martinez Jurado, Jessica, "Endocrine Disrupting Compound 4-Nonylphenol and Neurodegeneration" (2013). *Open Access Theses & Dissertations*. 1669.
https://digitalcommons.utep.edu/open_etd/1669

This is brought to you for free and open access by DigitalCommons@UTEP. It has been accepted for inclusion in Open Access Theses & Dissertations by an authorized administrator of DigitalCommons@UTEP. For more information, please contact lweber@utep.edu.

ENDOCRINE DISRUPTING COMPOUND 4-NONYLPHENOL AND

NEURODEGENERATION

JESSICA MARTINEZ JURADO

Department of Biological Science

APPROVED:

_____
Sukla Roychowdhury, Ph.D., Co-Chair

_____
Siddhartha Das, Ph.D., Co-Chair

_____
Elizabeth Walsh, Ph.D.

_____
Giulio Francia, Ph.D.

_____
Benjamin C. Flores, Ph.D.
Dean of the Graduate School

ENDOCRINE DISRUPTING COMPOUND 4-NONYLPHENOL AND NEURODEGENERATION

by

JESSICA MARTINEZ JURADO, B.S.

THESIS

Presented to the Faculty of the Graduate School of

The University of Texas at El Paso

in Partial Fulfillment

of the Requirements

for the Degree of

MASTER OF SCIENCE

Department of Biological Sciences

THE UNIVERSITY OF TEXAS AT EL PASO

December 2013

ACKNOWLEDGEMENTS

A major research project like this is never the work of only one person. The contributions of many different people, in their different ways, have made this possible. I would never have been able to finish my thesis without the guidance of my committee members, Dr. Das, Dr. Francia and Dr. Walsh. I would like to acknowledge Dr. Almeida and Dr. Arigi for helping me with their expertise in proteomic analysis.

I would like to express my deepest gratitude to my mentor, Dr. Sukla Roychodhury, for her excellent guidance, caring, patience, friendship and providing me with an excellent atmosphere for doing research. Indeed, without her guidance, I would not be able to put the topic together. Thank you.

Of course, this project would not have been possible without the participation of others. I would like to thank Ms. Gladys Almodovar for her support and help in cell culture and Dr. Varela for helping me with confocal analysis. Special appreciation goes to Jorge Sierra, who is a good friend and always willing to help and give his best suggestions. It would have been a lonely lab without him. I would like to give my appreciation to Amaris Castañón, Tania Medina and Michelle Carreón, and other workers in the laboratory for helping me with my research. My research would not have been possible without their help.

Also, I would like to thank my parents for their unconditional support, both financially and emotionally throughout my degree. In particular, the patience and understanding shown by my mother, father and my two brothers during these years is greatly appreciated. They were always supporting me and encouraging me with their best wishes. Last but not least, I would like to thank my husband. He was always there cheering me up and stood by me through the good times and bad.

ABSTRACT

Neurodegeneration, a progressive loss of nerve cells (neurons), occurs in many neurological disorders including Alzheimer's disease, Parkinson's disease, Schizophrenia, and drug addiction. Cytoskeletal disruption in neurons and aggregation of proteins associated with these disorders is the hallmark of neurodegeneration. However, the cause of neurodegenerative disorders is unknown and currently there are no effective drug treatments. Aging is the most consistent risk factor for developing a neurodegenerative disorder, and recent evidence suggests that environmental factors, which act as endocrine disruptors, pose a risk in the disease process. 4-nonylphenol (4-NP), an endocrine-disrupting compound (EDC), has been shown to affect brain development and may cause neurodegeneration. In the environment, 4-NP arises as a degradation product of alkylphenol polyethoxylates, compounds widely used as nonionic surfactants in commercial production, as well as in herbicides, pesticides, polystyrene plastics, and paints and has been shown to undergo high level of accumulation in biological tissues. However, the mechanism by which 4-NP exerts its effect is not understood. Recent results from our laboratory indicate that Gβγ, an important component of the G protein-signaling pathway, induces neurite outgrowth and that the interactions of Gβγ with microtubules (MTs), an important component of the cytoskeleton, is important for this process. Furthermore, we found that blocking the Gβγ-MT interaction induces neurodegeneration. The goal of the present research is to determine whether 4-NP inhibits neurite outgrowth and induces neurodegeneration by altering the Gβγ-MT-mediated pathway, and if other cytoskeletal components are involved in this process. Pheochromocytoma (PC12) cells were used to conduct the study because they respond to nerve growth factor (NGF) and exhibit a typical phenotype of neurons. In Specific Aim 1, using

biochemical, pharmacological, and immunoconfocal methodologies, I have demonstrated that 4-NP inhibits neurite outgrowth and induces neurodegeneration by altering MT-Gβγ interaction in PC12 cells. In Specific Aim 2, I have conducted the proteomic analysis of 4-NP treated cells and found that the compound affects the cytoskeletal profile in NGF-differentiated PC12 cells. In conclusion, I propose that one of the mechanisms by which 4-NP causes neuronal damage is by altering the Gβγ-cytoskeletal mediated pathway, which is critical for neuronal growth and development.

TABLE OF CONTENTS

LIST OF FIGURES

LIST OF TABLES

CHAPTER 1: INTRODUCTION

1.1. 4-Nolylphenol (4-NP)

There are established and increasing concerns of the potential health hazards caused by endocrine-disrupting compounds (EDCs), which are found in foods, pesticides, industrial chemicals, and consumer products. EDCs have adverse effects on wildlife, human health, and the environment. These compounds also play a role in disturbing homeostatic control and contribute to psychological disorders, cancer, and defects in reproductive, behavioral, and immune functions (Safe, 2000). 4-Nolylphenol (4-NP), one of the most prevalent EDC, is a synthetic organic chemical produced in relatively large quantities in the U.S. and used primarily in making detergents, pesticides, plastics, and rubber, as well as other commercial uses. Human exposure to 4-NP may occur through ingestion of contaminated foods, drinking water, and contact with detergents. 4-NP is an anaerobic breakdown product of nonylphenol ethoxylates (NPEOs), mixtures of non-ionic surfactants that are used in industrial and institutional cleaners, agricultural pesticides, and paint production (Figure 1.1). 4-NP has been detected in surface and ground water, sediments, aquatic organisms, wastewater effluent, air, and human food (California Environmental Protection Agency, 2009; U.S. Environmental Agency, 2010). Recent research has identified 4-NP as the most significant NPEO degradation product of because of its estrogenic toxicity, enhanced resistance toward biodegradation, and bioaccumulation in aquatic organisms (Lin, 2007), with a tissue concentration ranging from 1–20 μM (Bevan et al, 2006).

The most common route of NP entry into the environment is through wastewater. Because of its extensive use in cleansers, most NPEO are discharged to the sewer system and make their way into wastewater treatment plants. Under anaerobic conditions such as those

found in sewers, sediments, and certain treatment operations at wastewater treatment plants, NPEO are biodegraded to NP (Porter and Hayden, 2002). Residues of 4-nonylphenol have been reported in river water, groundwater adjacent to a contaminated river, seawater, tap water, sediments, and fish tissues [Hu, 2002]. Concentrations of 4-nonylphenol in surface waters are in the range of 0.11 to 180 micrograms per liter. (Tanghe and Verstraete, 2001). Rudel et al. found concentrations of NP greater than 1000 μg/L in numerous septic tank samples collected from Cape Cod, Massachusetts (Rudel et al, 1998). 4-Nonylphenol is hydrophobic, relatively insoluble in water, and can persist and accumulate in sediments and sludge. (Kim et al, 2005). It may take months or years to degrade in the environment.

NP is toxic to a wide variety of marine and freshwater vertebrate and invertebrate species in laboratory setting. Because of its potential environmental toxicity issues, European countries have restricted or banned the use of NPEO since 1980s (Renner, 1997). Because toxicity and risk at low concentrations have not been clearly proven, United States allowed its use. However, the level of risk to humans and the environment posed by 4-NP is currently under considerable debate by researchers, chemical manufacturers, and regulators. There are no existing regulations for 4-nonylphenol in drinking water; nor is the compound listed as a candidate for future regulatory decision-making.

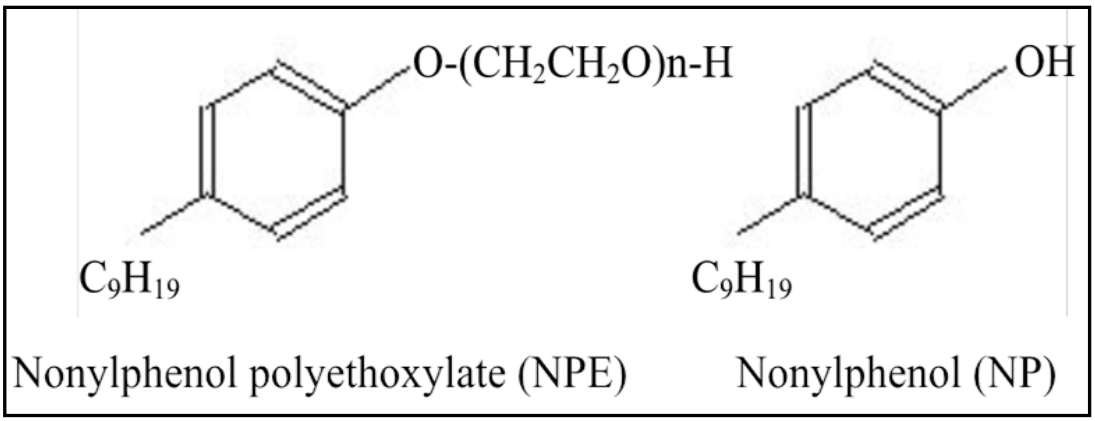

[Figure 1.1 Chemical structures of nonylphenol polyethoxylate and nonylphenol (Goto and Ibuki, 2004)]

1.2 4-Nolylphenol (4-NP) and Neurodegeneration.

4-NP, along with other EDCs, have been shown to induce a deterioration of neural development, a decrease in memory as well as learning capacity and spatial learning, and permanently alter hippocampus ultrastructurein in mice (Yoshikawa, 2005). Exposure to the compound also irreversibly influences monoaminergic neural pathways (Negishi et al, 2004). 4-NP been shown to inhibit neurotrophin-dependent neurite outgrowth in cultured embryonic *Xenopus* spinal-cord neurons and PC12 cells. Interestingly, the effect of 4-NP was not inhibited by the nuclear estrogen receptor (ER) antagonist (ICI182, 780), but was inhibited by the G-protein antagonist, pertussis toxin (Bevan et al, 2006). These data suggest that the effects of 4-NP are G-protein dependent and exposure may have a potentially damaging impact during early neuronal development. Other studies have exhibited that gestational 4-NP exposure can profoundly alter neurobehavioral development and reproductive development in male offspring and growth development in fetal rats (Jie et al, 2010). Studies conducted in neural stem cells suggest that 4-NP might directly cause neurodegeneration (Kudo et al, 2004). Taken together, these studies suggest that 4-NP can affect brain function, neuronal outgrowth, differentiation and development, and may cause neurodegeneration (California Environmental Protection Agency, 2009).

1.3 Neuronal Cytoskeleton, Neurite Outgrowth, and Neurodegeneration

Neurite outgrowth and differentiation is a complex process in which two distinct domains emerge from the cell body: a long, thin axon that transmits signals and multiple shorter dendrites that are specialized to receive signals. When fully differentiated through elongation of axon and dendrites, this morphology allows neurons to achieve precise connectivity between appropriate sets of neurons, which is fundamental to proper functioning of the nervous system. The cytoskeleton plays a key role in maintaining the highly asymmetrical shape of neurons that is characterized by neuronal outgrowth, branching, retraction, and guidance. Assembly and disassembly of microtubules (a major component of the cytoskeleton) is critical for axon and dendrite formation as well as for neurite outgrowth. Microtubules (MTs) form dense, parallel arrays in axons and dendrites that are required for the growth and maintenance of these neurites (Witte and Bradke; Geraldo and Gordon-Weeks, 2009). Selective stabilization of MTs also occurs during neuronal differentiation (Bulinsky and Gundersen, 1991). During neurodegeneration, the MT assembly and proteins associated with them are severely altered. Neurodegeneration, a progressive loss of nerve cells (neurons), occurs in many neurological disorders, including Alzheimer's disease (AD), Parkinson's disease (PD), and in the aging brain. In Alzheimer's disease, amyloid plaques and neurofibrillary tangles (NFT) comprise the two major neuropathologic brain alterations. NFT are formed from paired helical filaments (PHF) consisting of tau, a microtubule-associated protein (MAP). Under normal conditions, tau binds to MT, stabilizing neuron structure and integrity. In an AD brain, the MT structure is disrupted, which causes tau to be hyperphosphorylated and not bind to the MTs. Lewy bodies, which are considered cytopathological markers of Parkinson's disease (PD), are comprised of tubulins (subunit protein of MTs) MAP1, and MAP2 (Alonso et al., 2008; Amniai et al., 2008; Gustav et

al., 2010). Previously, the majority of research and drug-discovery efforts in the area of neurodegenerative diseases have focused on these pathological markers. Although this research has significantly advanced our understanding of the pathology of neurodegenerative disorders, the causes remain largely unknown. Most importantly, there are no effective drugs currently available to treat these neurodegenerative disorders, suggesting a critical knowledge gap in our understanding of how the diseases are triggered and then progress. Recent results suggest that MT assembly is severely compromised in both the AD and PD brains (Cash et al., 2003; Cartelli et al., 2010; Cartelli et al., 2013). This could play a significant role in triggering early disease phases, followed by the demise of neurons and neuronal death.

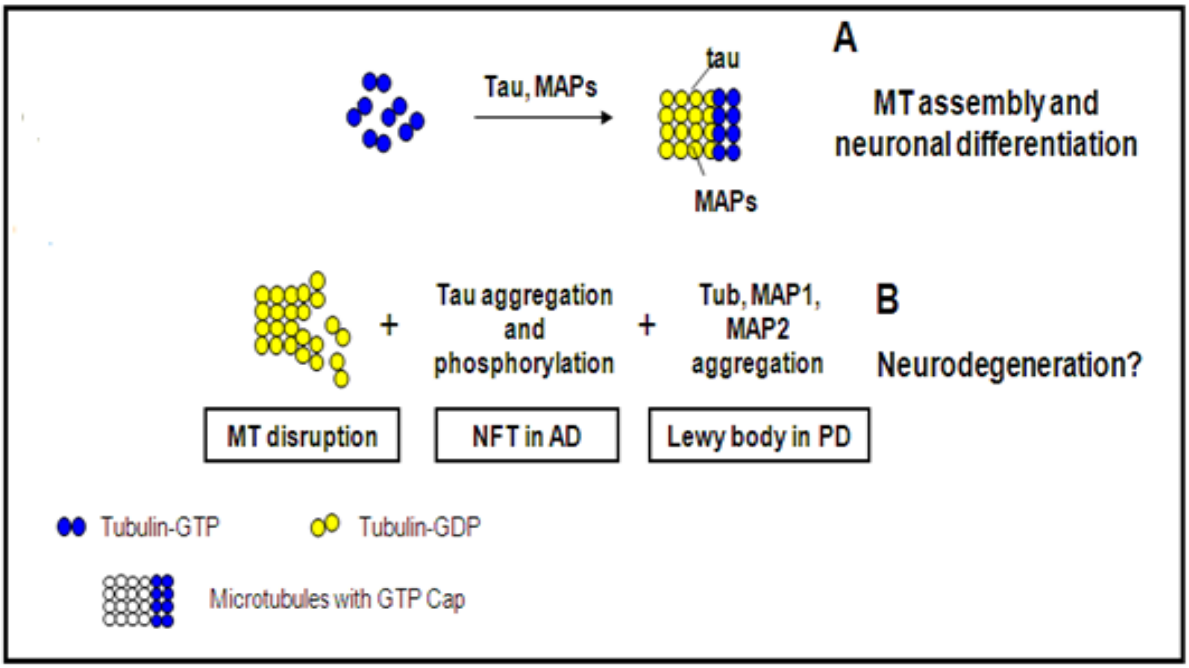

[Figure 2.1 MT assembly and its possible role in neurodegeneration**.** Irregular organization of the MT cytoskeleton is known to be a feature of neurodegeneration in Alzheimer's disease (AD) and Parkinson's disease (PD). Since Gβγ is known to have a role in the regulation of MT assembly, we propose that blocking the interaction of Gβγ with tubulin/MTs by 4-NP will alter MT organization in neuronal cell models and ultimately lead to neurodegeneration.]

1.4 Microtubule Assembly (MT) and G-Protein-Mediated Signaling

Previous studies from our laboratory have indicated that MT assembly could be regulated by G protein-mediated signaling (Roychowdhury and Rasenick, 1997; Roychowdhury et al., 1999; Roychowdhury et al., 2006; Montoya et al., 2007). G protein-mediated signaling, a major signaling pathway in neurons consists of three components; G protein-coupled receptors (GPCRs), G protein, and effector molecules. GPCRs constitute the largest family of transmembrane receptors and mediate the action of extracellular signals as diverse as light, odorants, peptide hormones, and neurotransmitters. All GPCRs have significant sequence resemblance to each other and share a similar topological motif comprised of seven hydrophobic segments that span the lipid bilayer. G proteins act as signal transducers and transfer signals from GPCRs to intracellular effector molecules. These effectors include adenylyl cyclase, phospholipase C, phospholipase A_2, and several ion channels (Figure 3.1).

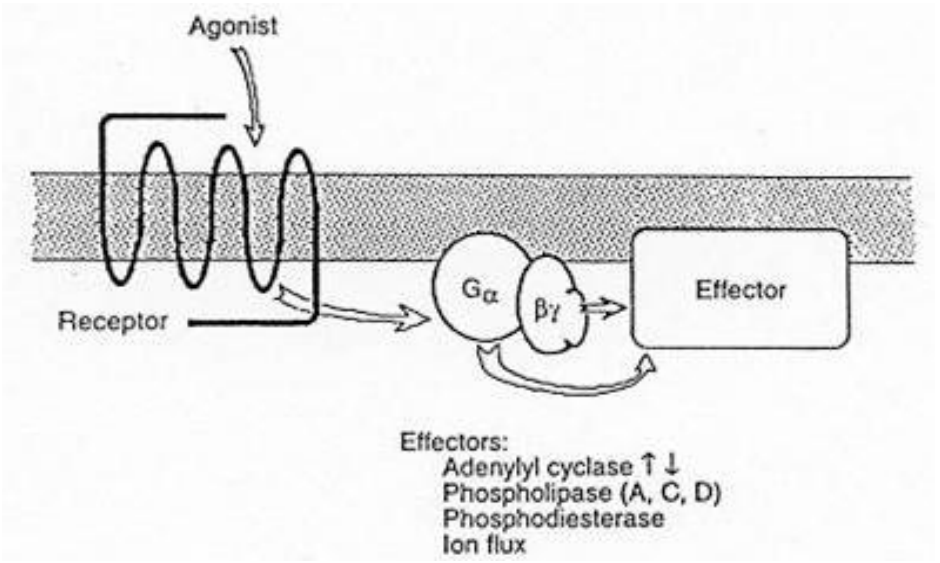

[Figure 3.1 Signal Transduction pathway. An agonist binds to a receptor activating the G-protein. The G-protein subunits (α and β γ) then dissociate and activate their respective effector molecules]

Current models of G proteins favor a heterotrimeric structure composed of the guanine-nucleotide binding α, plus β and γ subunits, the latter two forming a tight association under nondenaturing conditions. Agonist-bound receptors activate G proteins by allowing GTP to bind to the βγ subunit of the heterotrimer. Subsequently, activated Gα changes its association with Gβγ in a manner that allows both subunits to contribute to the regulation of intracellular-effector molecules (Figure 4.1). The α subunit has an intrinsic GTPase activity, which causes functional dissociation from the effector and reassociation with βγ. GPCR and heterotrimeric G proteins are abundant in neurons and involved in regulating neurite outgrowth (Igarashi et al., 1993; Reinoso et al., 1996; Lotto et al., 1999; He et al., 2005).

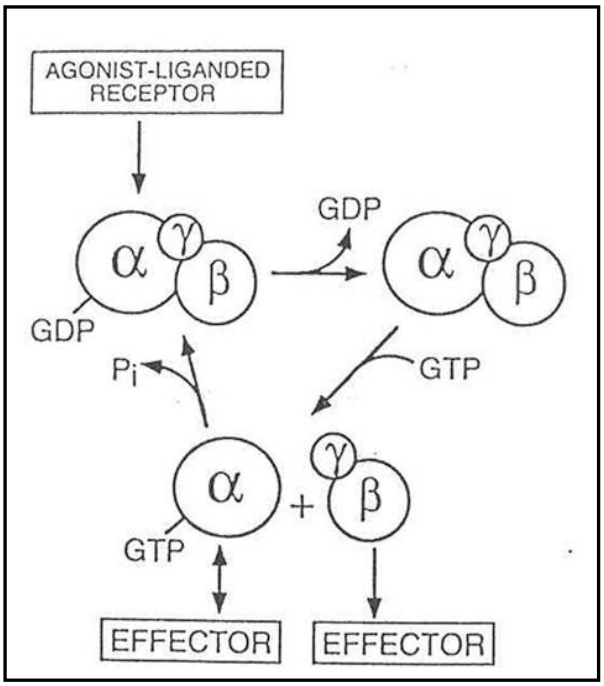

[Figure 4.1 G-protein activation cycle. When a ligand activates its receptor, heterotrimeric G-proteins are activated by dissociating into α and βγ subunits through GDP/GTP exchange mechanism.**]**

Evidence from our laboratory indicates that α and βγ subunits of G proteins regulate microtubule assembly *in vitro* (Roychowdhury and Rasenick, 1997; Roychowdhury et al., 1999; Roychowdhury et al., 2006; Montoya et al., 2007). While Gα activates tubulin GTPase and inhibits microtubule assembly, Gβγ promotes tubulin polymerization. Reconstituted heterotrimers were shown to be inactive in promoting microtubule assembly, which suggests that G-protein activation is necessary for the modulation of microtubules by G-protein subunits. Using the anti-mitotic agent nocodazole, it has been demonstrated that the assembly/disassembly of MTs alters tubulin-Gβγ interaction in cultured PC12 and NIH3T3 cells (Montoya et al., 2007). While MT depolymerization by nocodazole inhibited the interactions between tubulin and Gβγ, this inhibition was reversed when MT assembly was restored by the removal of nocodazole. The finding suggests that Gβγ might be involved in promoting MT assembly and/or stabilization of MTs *in vivo* as demonstrated *in vitro*. The stimulation of MT assembly in response to GPCR activation correlated with an increased association of Gβγ with polymerized tubulin, suggesting that GPCRs may utilize Gβγ to regulate MT assembly *in vivo* (Gutierrez, Sierra-Fonseca, Martinez-Jurado et.al, manuscript under preparation).

1.5 Gβγ-MT Association and Neurodegeneration

More recent studies from our laboratory show that Gβγ is critical for NGF-induced neuronal differentiation of PC12 cells (Sierra-Fonseca, Martinez-Jurado et.al, Manuscript under preparation). It was found that NGF-induced neurite outgrowth promoted the interaction of Gβγ with MTs and stimulated MT assembly. Furthermore, the Gβγ–sequestering peptide GRK2i inhibited neurite formation, disrupted MTs, and induced axonal damage. Because prenylation and subsequent methylation/demethylation of γ subunits are required for Gβγ-MTs interaction, we tested small-molecule inhibitors targeting prenylated-methylated protein methyl esterase (PMPMEase), and found that these inhibitors disrupted Gβγ and MT organization, affected cellular morphology, and inhibited neurite outgrowth. In further support of a Gβγ-MT interaction role in neuronal differentiation, it was observed that overexpression of Gβγ in PC12 cells induced neurite outgrowth in the absence of added NGF. Moreover, overexpressed Gβγ exhibited a pattern of association with MTs similar to that observed in NGF-differentiated cells. Altogether, results from our laboratory suggested that the G-protein complex Gβγ, initiated by the activation of the G protein-coupled receptor (GPCR), is a signal-transducing protein complex, and its interaction with microtubules (MTs) is important to neuronal development, differentiation, structure, and neurodegeneration (Figure 5.1).

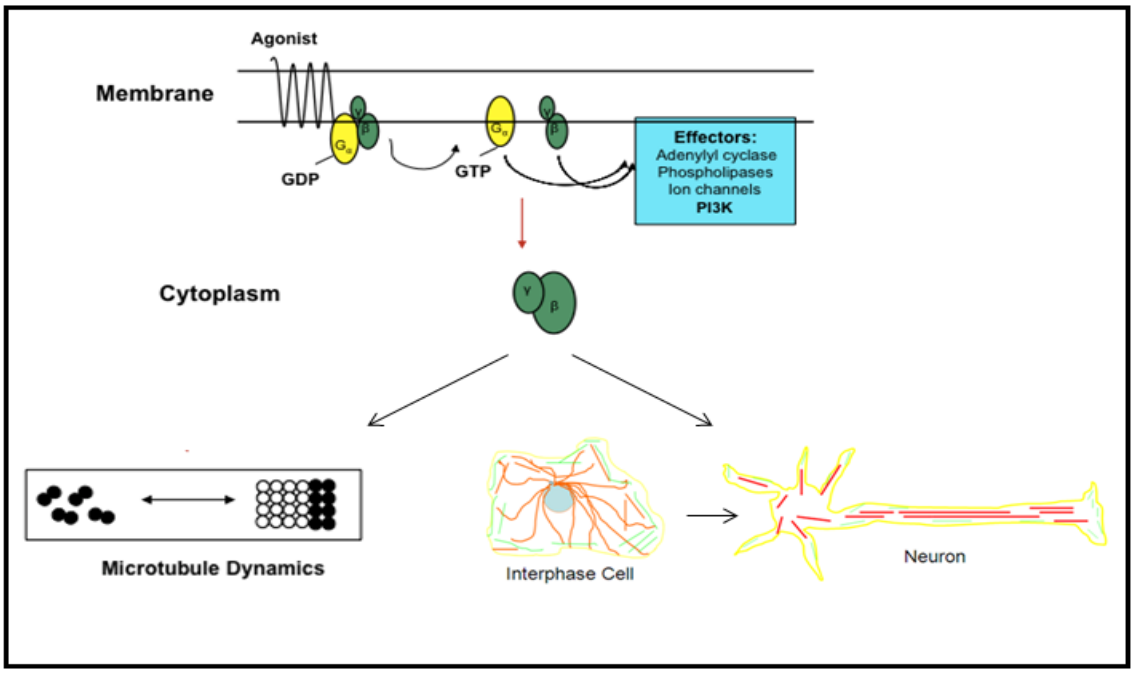

[Figure 5.1 Gβγ signaling, MT assembly, and Neurite outgrowth. GPCR transduce signals through heterotrimeric G-proteins. Upon activation, Gα dissociates from Gβγ subunits. Both subunits then activate signaling pathways such as ion channels, phospholipases, adenylcyclases, and PI3-kinases. Previous results from our lab have shown that Gβγ stimulates MT assembly, and induces neurite outgrowth from PC12 cells.

1.6 Hypothesis and Objective

The objective of my research is to understand the mechanism by which 4-NP, an endocrine-disrupting compound (EDC), induces neurodegeneration. *I hypothesize that 4-NP inhibits neurite outgrowth from PC12 cells and induces neurodegeneration by interfering with Gβγ-MT mediated pathways.* To test this hypothesis, experiments were conducted under two Specific Aims as described below.

- Specific Aim-1: Does 4-NP inhibit neurite outgrowth and differentiation, and induce neurodegeneration by interfering with the MT-Gβγ mediated pathway?
- Specific Aim-2: Does 4-NP alter the cytoskeleton and associated proteins to induce neurodegeneration?

These two Specific Aims are important in considering the physiological and toxicological significance of 4-NP in neurodegeneration.

CHAPTER 2: MATERIALS AND METHODS

2.1 Cell Culture, NGF and 4-NP Treatment. PC12 cells (pheochromocytoma cells derived from the adrenal gland of *Rattus norvegicus*) (ATCC, Manassas, VA) were grown in 75-cm^2 culture flasks at 37 °C in Dulbecco's Modified Eagle's Medium (DMEM) (4.5 g/L glucose, L-glutamine, without pyruvate), supplemented with 10% bovine calf serum and antibiotics (100 U/mL penicillin and 100 µg/mL streptomycin) in 10% CO_2. For NGF treatment, PC12 cells were grown on 100- or 150-mm plates to 70% confluence over 1–2 days. Then, cells were treated with 100 ng/ml of NGF (Sigma-Aldrich, St. Louis, MO) dissolved in complete media for 3 consecutive days. Control cells without NGF were also grown under the same conditions. Cells were treated with 4-Nonylphenol (sigma-aldrich, St. Louis, MO) at different concentrations (.2µM, 1µM, 5µM, 10µM and 50µM) for 1 hour. A stock solution of 10 mM 4-NP was prepared in DMSO and diluted in tissue culture media to a final concentration of 1, 5 or 10 µM 4-NP and added to the cells as indicated in the figures. The DMSO concentration in the culture media never exceeded 0.1%. Besides, control experiment was performed in the presence of similar concentration of DMSO.

2.2 Extraction of Cytoskeletal (CSK) and Soluble Protein (SOL) Fractions. PC12 cells were grown in 100- or 150-mm plates to 70% confluence over 1–2 days and subjected to NGF treatment as described above. The plates were used in duplicates for each condition. Subsequently, the plates were treated with or without 4-NP for 1 hour. Cytoskeletal (CSK) and soluble (SOL) fractions were prepared by extracting soluble proteins in an MT -stabilizing buffer (MS). The stabilizing buffer contained 0.1 M PIPES, pH 6.9, 2 M glycerol, 5 mM $MgCl_2$, 2 mM EGTA, 0.5% Triton X-100, protease inhibitor cocktail (Sigma-Aldrich), 0.1 mM GTP, and 1 mM DTT. Briefly, cells were rinsed and incubated with MS buffer (0.5–1 ml) for ~10 minutes at

room temperature until cells were beginning to lyse. Subsequently, cells were removed mechanically (using a cell scraper) and centrifuged at 10,000 × g for 10 min. The supernatant constitutes the SOL fraction, and the cell pellets represent the CSK fraction that includes the tubulin polymers. Cytoskeletal pellets were washed and resuspended in 0.25 mL PEM (0.1 M PIPES, pH 6.9, 0.5 mM $MgCl_2$, 1 mM EGTA) buffer, kept on ice for 15 min to depolymerize the MTs, sonicated on ice for 1 min, and clarified by centrifugation. The protein concentration of the samples was determined using the Bio-Rad protein assay, using bovine serum albumin (BSA) as a standard.

2.3 Preparation of Whole-cell Extracts. PC12 cells were grown in 100-mm or 150-mm plates to 80% confluence over 1–2 days. Cells were then treated with or without 4-NP as indicated. The medium was then removed and the cells were washed first with PBS and then with 0.5–1 mL lysis buffer (10 mM Tris-HCl, pH 7.9, 1.5 mM $MgCl_2$, 0.3 M sucrose, 1 mM DTT and protease inhibitor cocktail). Cells were scraped with a cell scraper, sonicated for 1 min, followed by centrifugation at 10,000 × g for 10 min. Supernatants represent whole-cell protein extracts. Protein concentrations were typically between 1–2 mg/mL.

2.4 Immunoprecipitation. For immunoprecipitation, 100–200 µL aliquots of cellular fractions (~0.25–1 mg/mL) were incubated with or without anti-Gβ-protein specific antibody (rabbit polyclonal anti-Gβ, Santa Cruz Biotechnology, Santa Cruz, CA) for 1 h at 4 °C, followed by the addition of 100 µL 50% protein A-sepharose (Amersham Biochemical, Piscataway, NJ), pre-equilibrated in 10 mM Tris-HCl, pH 8.0 at 4 °C, overnight. Samples were then centrifuged at 10,000 × g for 6 min, and the supernatants (SUP) were saved. The pellets (immunocomplex) were washed with PBS, eluted with 3% SDS Laemmli sample buffer containing 0.15 M dithiothreitol (DTT), and boiled in a water bath for 5 min. Samples were then clarified by

centrifugation and they represented immunoprecipitants (IP). Both IP and SUP fractions were subjected to immunoblotting using anti-α-tubulin (DMIA, mouse monoclonal from Sigma-Aldrich).

2.5 Electrophoresis and Immunoblotting. Samples for immunoblotting were subjected to SDS-polyacrylamide gel (10%) electrophoresis, followed by electrotransfer onto nitrocellulose membranes. The membranes then were incubated in 5% non-fat dry milk in TBS (10 mM Tris-HCl and 150 mM NaCl, pH 7.4) for 1 hour at room temperature, followed by an overnight incubation with anti-Gβ or anti-tubulin antibodies (1:250) in TBS containing 0.01% BSA. The membranes were washed with 0.05% Tween-20 in TBS (TBST) and incubated with the appropriate HRP-conjugated secondary antibodies (goat anti-mouse and goat anti-rabbit from Promega (Madison, WI), (1:1000) in TBST containing 0.01% BSA for 1 h at room temperature. For sensitive detection, the chemiluminescence (ECL) technique (SuperSignal West Pico Chemiluminescent Substrate) was used according to the manufacturer's (Pierce Biotechnology, Rockford, IL) instructions. Quantitative analysis was done using LabWorks image acquisition and analysis software (UVP Laboratory Products, Upland, CA).

2.6 Confocal Microscopy. For confocal microscopic analysis, PC12 cells were allowed to attach to immunocytochemistry slides (Lab-TEK II mounted on glass slides, VWR) and were grown overnight in DMEM with bovine calf serum and penicillin-streptomycin as described above. Cells were then treated with or without NGF, and subsequently fixed by the addition of ice-cold 100% methanol (previously cooled to -20 °C) and incubated at -20 °C for 6 min. The cells were then rinsed three times in 1% NGS in PBS and blocked for 1 h at room temperature in 5% normal goat serum (NGS) (Sigma-Aldrich) in PBS, followed by an overnight incubation at 4 °C with primary antibodies (mouse monoclonal anti-tubulin, and/or rabbit polyclonal anti-Gβ) in

PBS containing 1% NGS. The slides were rinsed as before and incubated for 2 h with the appropriate secondary antibodies (rhodamine-conjugated goat anti-mouse, fluorescein-conjugated goat anti-rabbit, and Alexa Fluor 350 donkey anti-goat, Molecular Probes-Invitrogen, Carlsbad, CA) in the dark to diminish photo-bleaching effects. The slides were then rinsed, mounted with DAKO mounting media (DAKO Corp., Carpenteria, CA), and covered with coverslip. High resolution, digital, fluorescent images were captured employing inverted, confocal laser scanning microscopy (model LSM 700; Zeiss, New York), utilizing a Plan-Apochromat 63x/1.40 immersion-oil DIC objective and assisted with ZEN 2009 software (Zeiss, New York, NY). Alexa Fluor 350 (blue), FITC (green), and rhodamine (red) were excited with laser emissions at 405-, 488-, and 555-nm wavelengths, respectively.

2.7 Overexpression of Gβγ. PC12 cells were transiently co-transfected with YFP-tagged pcDNA3.1 plasmids encoding for Gβ1 and Gγ2 subunits. The expression plasmids were provided by Dr. N. Gautam (Washington University, St. Louis). A plasmid encoding only YFP (pcDNA3-YFP, Addgene, Cambridge, MA) was used as control. The plasmids were transfected separately (Gβ1, and Gγ2), or co-transfected to generate the Gβ1γ2 combinations. Cells were transfected with the plasmids using Lipofectamine LTX PLUS reagent (Invitrogen) according to the manufacturer's instructions. Briefly, PC12 cells were seeded on glass coverslips using 12-well plates at a density of 50,000 cells/well, and they were incubated overnight under normal growth conditions. The following day, the cells were transfected with a mixture of Lipofectamine LTX PLUS containing 2 µg of each plasmid dissolved in antibiotic-free media and incubated under normal conditions overnight. Cells were monitored for protein expression (YFP fluorescence) and for morphological changes using differential interference contrast (DIC) images at different time points (24, 48, and 72 h), using a Zeiss Axiovert 200 fluorescence

microscope equipped with a GFP filter. For confocal microscopic analysis, the cells were fixed and processed as described above (confocal microscopy).

2.8 Differential nuclear staining (DNS) assay for cytotoxicity. To determine the levels of cytotoxicity caused by the 4-NP, a previously described DNS assay adapted for high-throughput screening was used (Lerma et. al., 2011). This assay uses two fluorescent nucleic acid intercalators, Hoechst 33342 (Hoechst) and propidium iodide (PI). Briefly, PC12 cells were seeded in a 96-well plate format and incubated with NGF and 4-NP. One h before image capturing, cells were added with a staining mixture of Hoechst and PI at a final concentration of 1 µg/mL for each dye. Subsequently, cells were imaged in live-cell mode using a BD Pathway 855 Bioimager system (BD Biosciences, Rockville, MD). Montages (2x2) from four adjacent image fields were captured per well in order to acquire an adequate number of cells for statistical analysis, utilizing a 10x objective. To determine the percentage of dead cells from each individual well, both image acquisition and data analysis were performed using the BD AttoVision v1.6.2 software (BD Biosciences), and each experimental condition was assessed in triplicate.

2.9 Neurite outgrowth assessment. For neurite outgrowth measurement, cells were fixed and processed for confocal microscopy using a mouse monoclonal anti-tubulin antibody and a rabbit polyclonal Gβ antibody, followed by labeling with rhodamine- and FITC-conjugated secondary antibodies. Due to the fast photo-bleaching of the FITC fluorophore, the cells were only imaged using rhodamine staining for the purpose of neurite outgrowth assessment. Cells were viewed using the 40x objective with a Zeiss LSM 700 confocal microscope. The coverslips were scanned from left to right, and 8–10 fields were randomly selected. For each field, neurites were traced and measured using the 2009 ZEN software (Zeiss), and at least 100 cells from three

independent experiments were scored for each condition. A cell was considered as neurite-bearing if it contained at least one neuronal process that was longer than the cell body.

2.10 Statistical analysis. All statistical analysis was performed using Sigma Plot 11 software. In the case of Western-blot quantitative analysis, the differences between controls and treatments were assessed by means of the student's paired t-test. For comparisons between two groups, the student's paired t-test was employed. In all cases, a value of $p < 0.05$ was considered to be statistically significant.

2.11 Sample Preparation for Proteomic analysis. PC12 cells were grown on four 100-mm plates to 80% confluence over 2 days. Subsequently, plates were then treated with (3 and 4) or without (plates 1 and 2) NGF for two consecutive days, followed by treatment with (plates 2 and 4) 10 μM 4-NP and NGF for an additional day, while the remaining plates (plates 1 and 3) were treated only with NGF and served as controls. The Cytoskeletal (CSK) and soluble (SOL) fractions were then prepared by extracting soluble proteins in an MT -stabilizing buffer (MS). The stabilizing buffer contained 0.1 M PIPES, pH 6.9, 2 M glycerol, 5 mM $MgCl_2$, 2 mM EGTA, 0.5% Triton X-100, protease inhibitor cocktail (Sigma-Aldrich), 0.1 mM GTP, and 1 mM DTT. Briefly, cells were rinsed and incubated with MS buffer (0.5–1 ml) for ~10 min at room temperature until cells were beginning to lyse. Subsequently, cells were removed mechanically (using a cell scraper) and centrifuged at 10,000 × g for 10 min. The supernatant constitutes the SOL fraction, and the cell pellets represent the CSK fraction.

2.11.1 LC–MS/MS analysis: Protein pellets were re-suspended in 100 uL 0.4 M NH4HCO3 containing 8M urea and reduced with 5 mM DTT for 30 min at 55°C. Reduced thiol groups were alkylated with 10 mM iodoacetamide for 30 min at room temperature, and diluted 8 fold to a

final concentration of 1M urea, 50mM NH_4HCO3. The samples were digested overnight at 37°C with sequencing grade trypsin (Sigma-Aldrich). After quenching the reaction with TFA to a final concentration of 0.05% TFA, the samples were desalted with 100mg C18 cartridges (Supelco) and dried in a vacuum centrifuge.LC–MS/MS analyses were performed on an Ultimate 3000 RSLCnano system online coupled to a Q-exactive (Thermo Scientific). Peptides were introduced to the analytical column (Acclaim® PepMap RSLC, 75 µm × 15 cm, nanoViper, C18, 2 µm, 100 Å) and separated using a 90 min gradient from 5 to 40% solvent B at a flow rate of 300 nl/min (solvent A: 0.1% formic acid 5 % acetonitrile, solvent B: 0.1% FA 80% acetonitrile). The mass spectrometer was operated in a data-dependent mode. Full scan MS spectra were acquired at a mass resolution of 70,000 (mass range 400–1600 *m/z* and a target value of 1E6) in the Orbitrap analyzer. Tandem mass spectra of the 10 most abundant peaks of a full scan MS spectrum were acquired following peptide fragmentation using higher-energy collisional dissociation (HCD) at a mass resolution 17,500 (target value of 2E5, NCE 28%, isolation width 4 *m/z*). The dynamic exclusion time was 15 s.

2.11.2 Protein identification: Protein identifications were performed with Proteome Discoverer software. Briefly, raw-files were searched against UniProtKB/Swiss-Prot database (taxonomy rat and common contaminant proteins) using Sequest. For database searches, mass tolerances were set to 10 ppm and 0.02 Da for precursor and fragment ions, respectively. For analyses two trypsin missed cleavages were allowed, modifications of cysteine (carbamidomethyl, static), methionine (oxidation, variable) and asparagine, glutamine (deamidation, variable) were considered. Confidence of peptide identifications was determined using percolator function, in Proteome Discoverer. Peptide identifications with false discovery rates > 1% (q-value > 0.01) were discarded.

CHAPTER 3: RESULTS

3.1 Specific Aim-1: Does 4-NP inhibit neurite outgrowth and differentiation and induce neurodegeneration by interfering with the MT-Gβγ mediated pathway?

3.1.1 Objective and Overview

Dynamic rearrangements of MTs are critical for growth-cone motility and neurite outgrowth. Previous studies have shown that the βγ subunit of signal-transducing G proteins promotes MT assembly (Roychowdhury and Rasenick, 1997; Roychowdhury et al., 1999; Roychowdhury et al., 2006; Montoya et al., 2007; Roychowdhury and Rasenick, 2008). More recently, it was found that NGF-induced neuronal differentiation of PC12 cells promotes the interactions of Gβγ with MTs and stimulated MT assembly. Overexpression of Gβγ in PC12 cells induced neurite formation in the absence of NGF. Furthermore, the Gβγ–sequestering peptide GRK2i inhibited neurite formation, disrupted MTs, and induced axonal damage (Sierra-Fonseca, Martinez-Jurado et. al., Manuscript under preparation), suggesting that the Gβγ-MT mediated pathway played a critical role in inducing neurite outgrowth and neurodegeneration. Because 4-NP has been shown to block NGF-induced neurite outgrowth, in Specific Aim-1 I examined the role of 4-NP in dynamic interactions between Gβγ and MTs during neuronal outgrowth and differentiation, using PC12 cells. NGF-induced neuronal differentiation, as well as overexpression of Gβγ, was used to address whether NP interferes with Gβγ-MT mediated pathways.

3.1.2 4-NP inhibits NGF-induced neuronal differentiation of PC12 cells and induces cellular aggregation and degeneration by altering the Gβγ-MT association

To determine the role of 4-NP on neurite outgrowth and development, we tested the effects of 4-NP on NGF-induced neuronal differentiation of PC12 cells using confocal microscopy. PC12 cells were allowed to attach in immunocytochemistry slides and grow overnight as indicated in the methods. Cells were then treated with or without NGF for three consecutive days to induce neuronal differentiation. Subsequently, cells were treated with or without 4-NP for 1 h and subjected to confocal miscopy as indicated in the methods. Tubulin was detected with a monoclonal, anti-tubulin antibody (red), Gβγ was identified with rabbit polyclonal anti-Gβ antibody (green), and DAPI staining (blue) represented nuclear labeling (Figure 6.1). Areas of co-localization between MTs and Gβγ appear yellow. As indicated in the figure, in the control-PC12 cells (in the absence of NGF) Gβγ were co-localized with MTs mainly in the perinuclear region and those cells displayed typical morphology (Figure 6.1, upper panel). After NGF treatment, Gβγ co-localized with MTs in both the cell body and the neuronal processes (Figure 6.1, lower panel). In the presence of 4-NP at 1 μM, the lowest concentration used, there are some noticeable morphological changes. Cells started to shrink and neurites shortened in comparison to the control cells. Consequently, at a concentration of 5 μM, aggregation of cells occurred and neurites were absent in most cells (Figure 7.1). At a higher concentration, 10 μM, 4-NP had more profound effects on blocking neurite formation and cellular degeneration, as expected. Many cells lost their shapes, processes were curly, and absent nucleus and cell aggregation was observed (Figure 7.1).

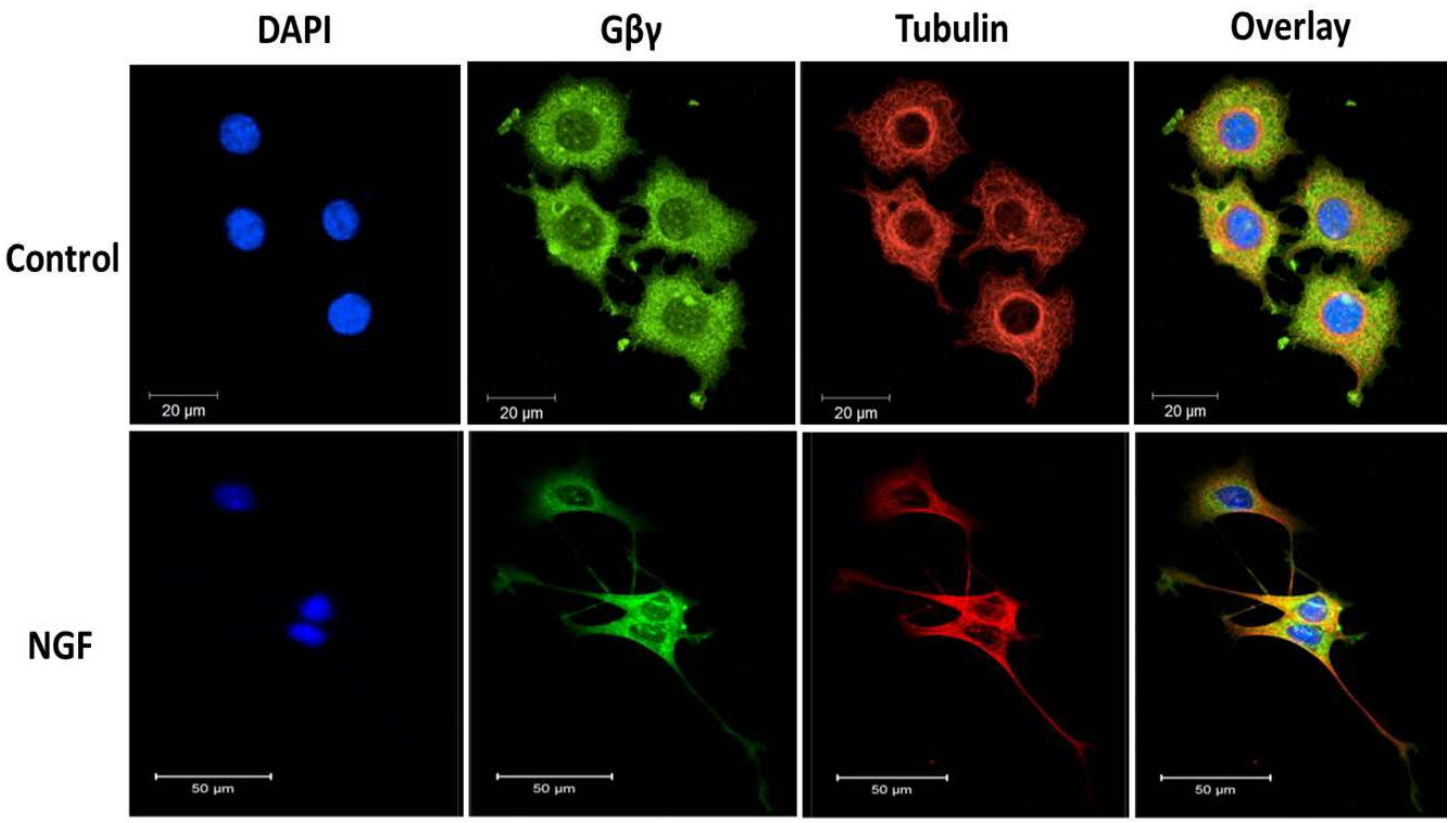

[Figure 6.1 NGF-Induced Neuronal differentiation of PC12 cells: Co-localization of Gβγ with MT in the neuronal processes. PC12 cells were treated with 100 ng/ml NGF for three consecutive days to induce neuronal differentiation. Samples were then fixed and stained with mouse monoclonal anti-tubulin and rabbit polyclonal anti-Gβ antibodies. Co-localization patterns of Gβγ (green) and tubulin (red) are shown by double immunofluorescence labeling. Blue represents nuclear labeling. In NGF treated cells, neurite outgrowth was observed. Co-localization between MTs and Gβγ (yellow) was observed mainly in the neuronal processes].

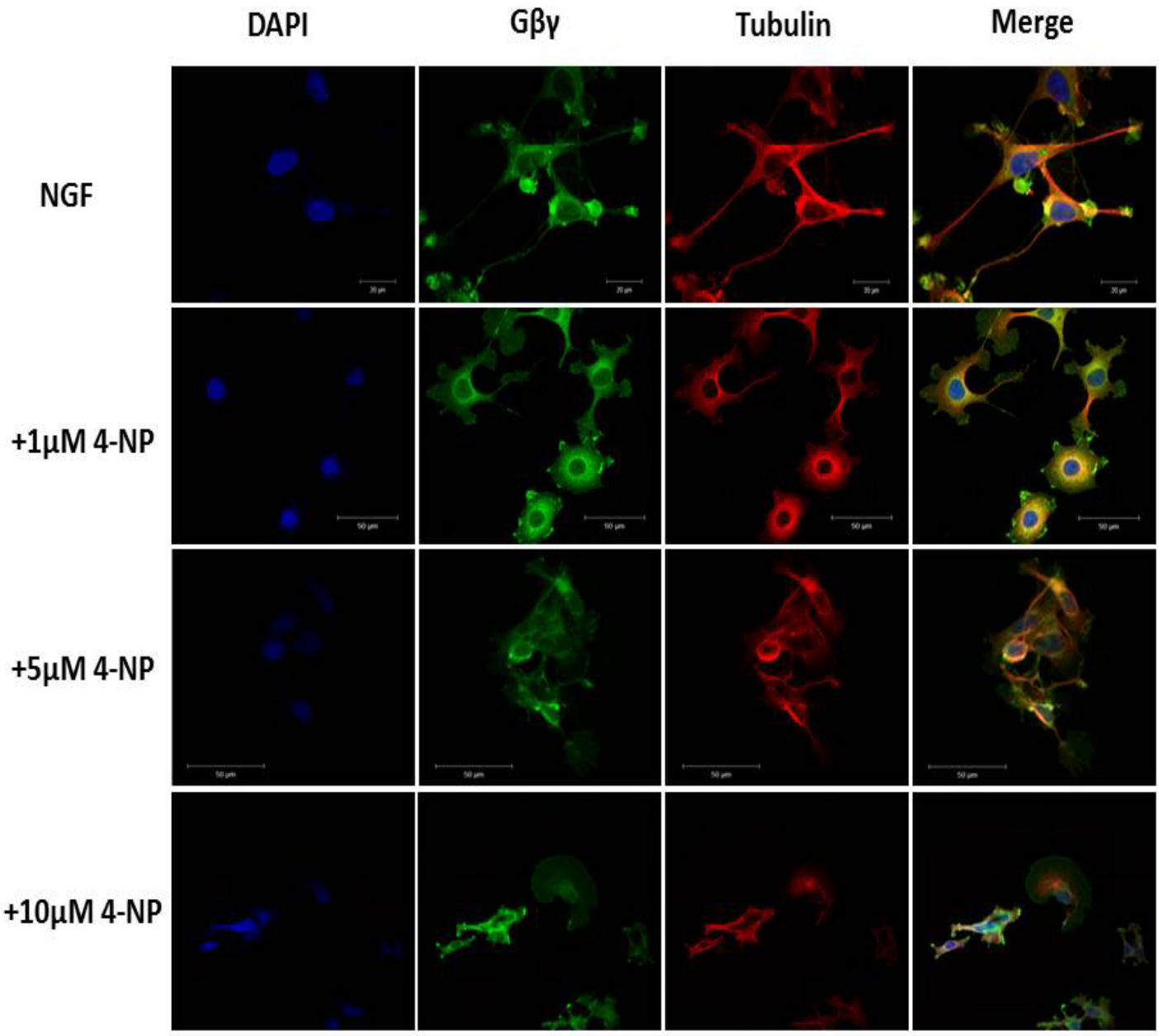

[Figure 7.1 Effect of 4-NP on NGF-Induced Neuronal differentiation of PC12 cells**.** PC12 cells were treated with 100 ng/ml NGF for three days to induce neuronal differentiation. Cells were then treated with 4-NP at 1μM, 5μM and 10μM. Samples were then fixed and stained with mouse monoclonal anti-tubulin and rabbit polyclonal anti-Gβ antibodies. Co-localization patterns of Gβγ (green) and tubulin (red) are shown by double immunofluorescence labeling. Blue represents nuclear labeling. In NGF treated cells, neurite outgrowth was observed. Co-localization between MTs and Gβγ (yellow) was observed mainly in the neuronal processes].

3.1.3 Neurite-outgrowth assessment after 4-NP treatment

Measurement of the number and length of neurites provided a quantitative assessment of neuronal differentiation. Therefore, the effect of 4-NP on neuronal differentiation was assessed by measuring average neurite lengths as well as the percentage of cells bearing neurites (Figure 8.1). To accomplish this, neurites were traced and measured using the 2009 ZEN software from Carl Zeiss, Inc. (Thornwood, NY). At least 100 cells from three independent experiments were scored for each condition in this assessment. A cell was considered neurite-bearing if it contained at least one neuronal process that was longer than the cell body (X μm in diameter). As indicated in Figure 8.1A, the percentage of cells bearing neurites was reduced significantly—from 55% in the control cells to 20% after 30 min of incubation with 1 μM 4-NP and further reduced to 5% in the presence of 5 μM 4-NP. Interestingly, the average neurite length of surviving neurites did not decease in the presence of 4-NP (Figure 8.1B). In fact, in the presence of 5 μM 4-NP, the average neurite length was found to be increased. This suggests that NGF-induced neurites are not equally susceptible to 4-NP, and a population of differentiated cells with longer neurites are resistant to 4-NP.

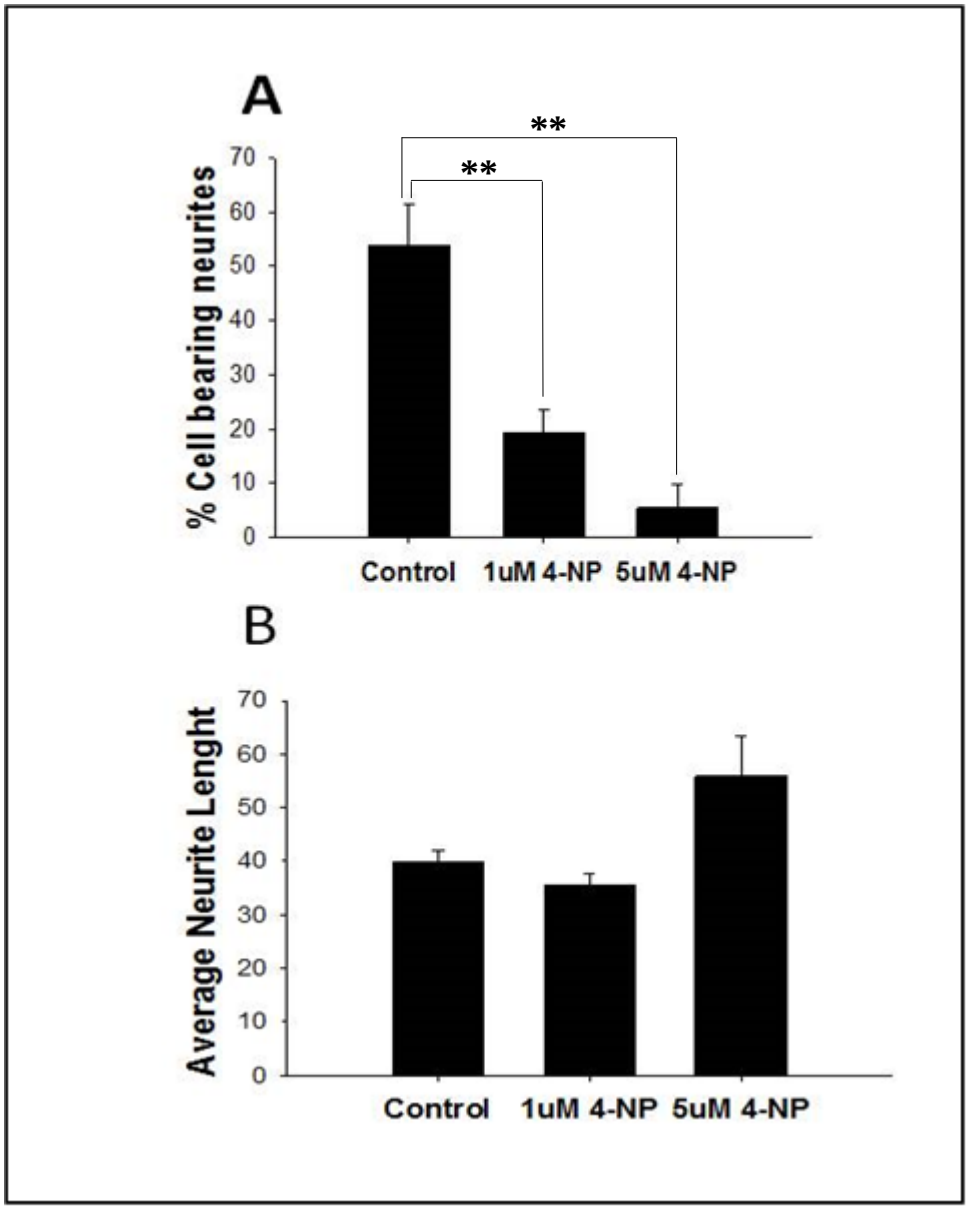

[Figure 8.1 Assesment of neurite outgrowth after 4-NP treatment. PC12 cells were treated with 100 ng/ml NGF for three days to induce neuronal differentiation. Cells were then treated with 1μM, and 5μM 4-NP followed by fixing and processing for confocal microscopy as described previously. Using the Zeiss ZEN software, neurites were traced and measured and expressed as percent of cells bearing neurites (A) and average neurite length (B). Differences between experimental conditions were assessed by one-way ANOVA. **$p < 0.001$]

3.1.4 Overexpression of Gβγ in PC12 cells induces neurite outgrowth in the absence of NGF; 4-NP inhibits this process and promotes neurodegeneration

Recently, our laboratory has shown that the overexpression of Gβγ induces neurite outgrowth from PC12 cells in the absence of NGF (Sierra-Fonseca, Martinez-Jurado et al., Manuscript under preparation). Therefore, to confirm the role of 4-NP in blocking neuronal differentiation and inducing neurodegeneration, we overexpressed Gβγ in PC12 cells. To accomplish this, PC12 cells were co-transfected with Gβ1 and Gγ2. YFP-tagged Gβ1 and Gγ2 constructs (YFP-Gβ1 and YFP-Gγ2) were used for transfection. A plasmid encoding just YFP was used as control. Cells were monitored for protein expression and possible neurite formation at different time points (24 h and 48 h). Within 24 h of transfection, β1γ2-transfected PC12 cells were found to overexpress the proteins as indicated by green fluorescence. At 48 h of transfection, YFP-β1γ2-transfected cells induced neurite formation in the absence of NGF (Figure 9.1**,** control). Cells were then treated with 4-NP (.2 μM, 1 μM or 10 μM) for 1 hour, and fixed and processed for confocal microscopy using anti-tubulin antibody (red). At a lower concentration, 4-NP (0.2 μM) displayed an absence of neurites and disruption of cells barely started to show. In the presence of 1 μM 4-NP, cellular aggregation as well as cell disruption occurred. As expected, 4-NP at a concentration of 10μM was most effective. Cellular aggregation, cell disruption, and nuclear damage were clearly visible at 10 μM 4-NP (Figure 9.1).

From confocal microscopic examination, I conclude that 4-NP inhibits Gβγ-induced neuronal differentiation of PC12 cells and induces neurodegeneration.

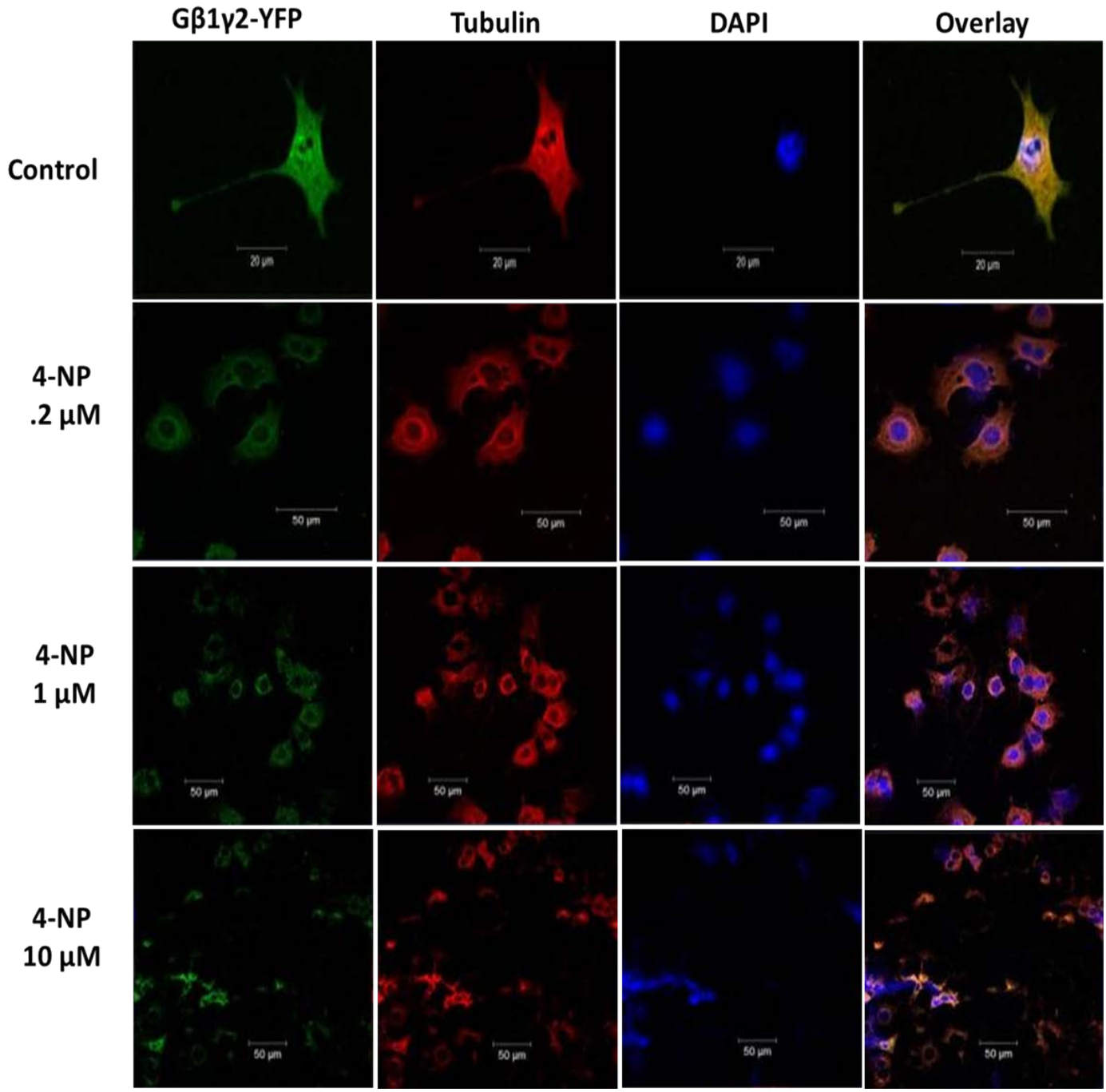

[Figure 9.1 Overexpression of Gβγ induces neurite outgrowth: 4-NP inhibits this process. PC12 cells were co-transfected with YFP-tagged Gβ1 and Gγ2 (β1γ2), using Lipofectamine LTX PLUS reagent. A construct encoding only YFP tag was used as control. Cells were treated at different concentrations with NP and morphological changes were observed using a fluorescence microscope.]

3.1.5 4-NP does not affect MT assembly but increases tubulin expression significantly

To understand the role of 4-NP and its link to MT assembly, we evaluated the effect of 4-NP in PC12 cells. To conduct the experiment, PC12 cells were treated with or without 10μM 4-NP. Cytoskeletal (CSK, enriched in MTs) and soluble protein fractions (SOL, enriched in dimeric tubulin) were separated as indicated in the methods. Tubulin immunoreactivity was measured in both fractions, and MT assembly was assessed by calculating the % of Tubulin in CSK fraction. We found that MT-assembly was not significantly decreased in PC12 cells after treatment at 10μM 4-NP (Figure 10.1). Treatment with 4-NP decreased MT assembly from 43.52% in control cells to 41.52% in treated cells. Previous studies indicated that Gβγ associates with microtubules and this association is important for microtubule assembly (Roychowdhury and Rasenick., 1997; Montoya et. al., 2007). Therefore we determined if Gβγ association with MTs were alter after 4-NP treatment. We found that 47.5% Gβγ was associated with MTs and 4-NP did not have any significant effect on this association.

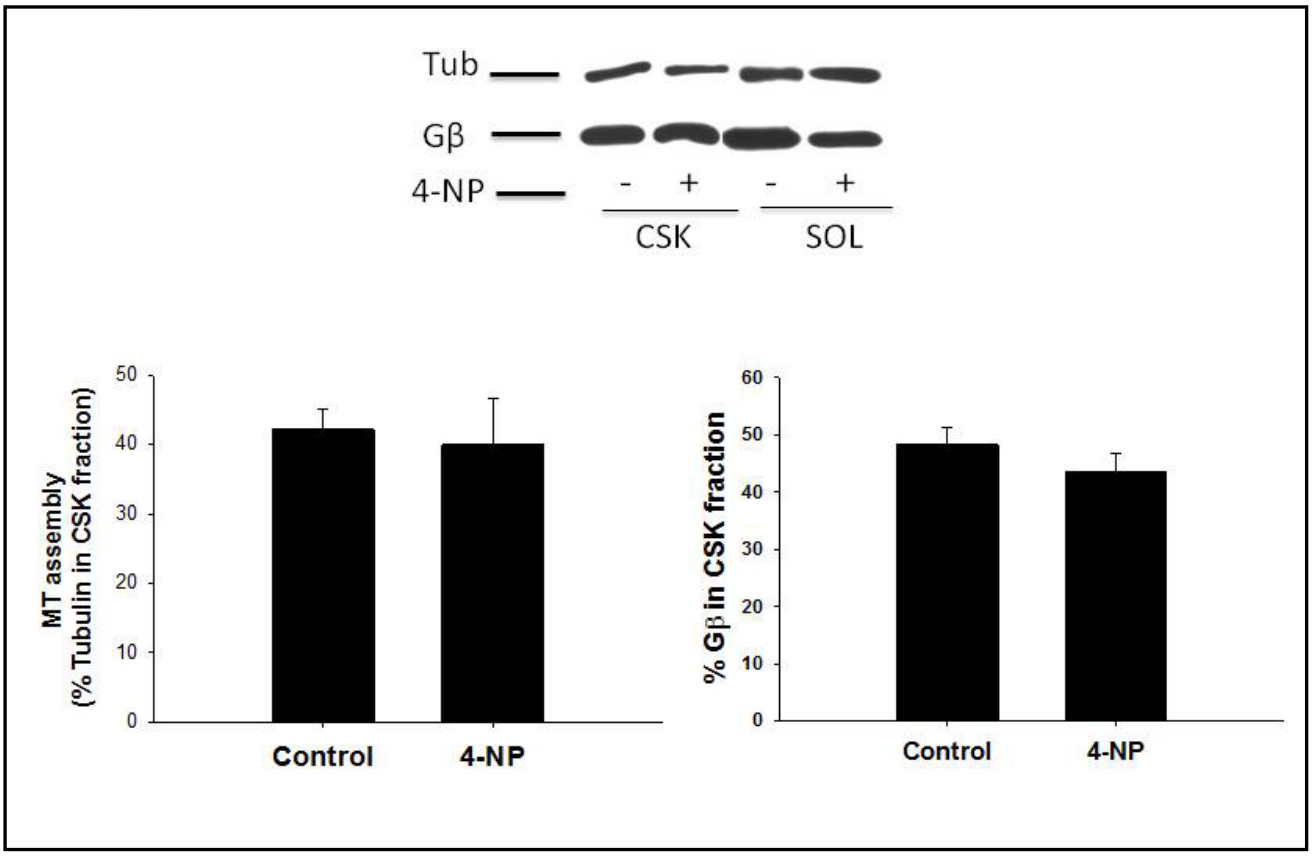

[Figure 10.1 Effect of 4-NP on MT assembly. PC12 cells were treated with 4-NP at a concentration of 10μM for 1 hour. After incubation, subcellular fractionation was performed and CSK and SOL fractions were subjected to Western blot using anti-tubulin antibody as indicated in the methods. Protein bands were detected using the ECL-plus reagent, quantitated. MT assembly was determined by assessing tubulin immunoreactivity in both fractions, and it is expressed as percent tubulin in CSK fraction. The graphic shows percent tubulin in CSK fractions. A representative experiment is shown. Values shown represent mean ± standard error of two independent experiments done in duplicates. No significant change was found]

To determine if 4-NP affected tubulin or Gβγ expression in the PC12 cells, we performed a whole-cell lysate extraction after treatment with 4-NP. The samples were processed for western blotting using anti-tubulin and anti-Gβ antibodies as described in the methods. As indicated in

the figure (Figure 11.1A) tubulin expression was significantly increased in the presence of 4-NP, while Gβγ expression remained unaltered after 4-NP treatment (Figure 11.1B).

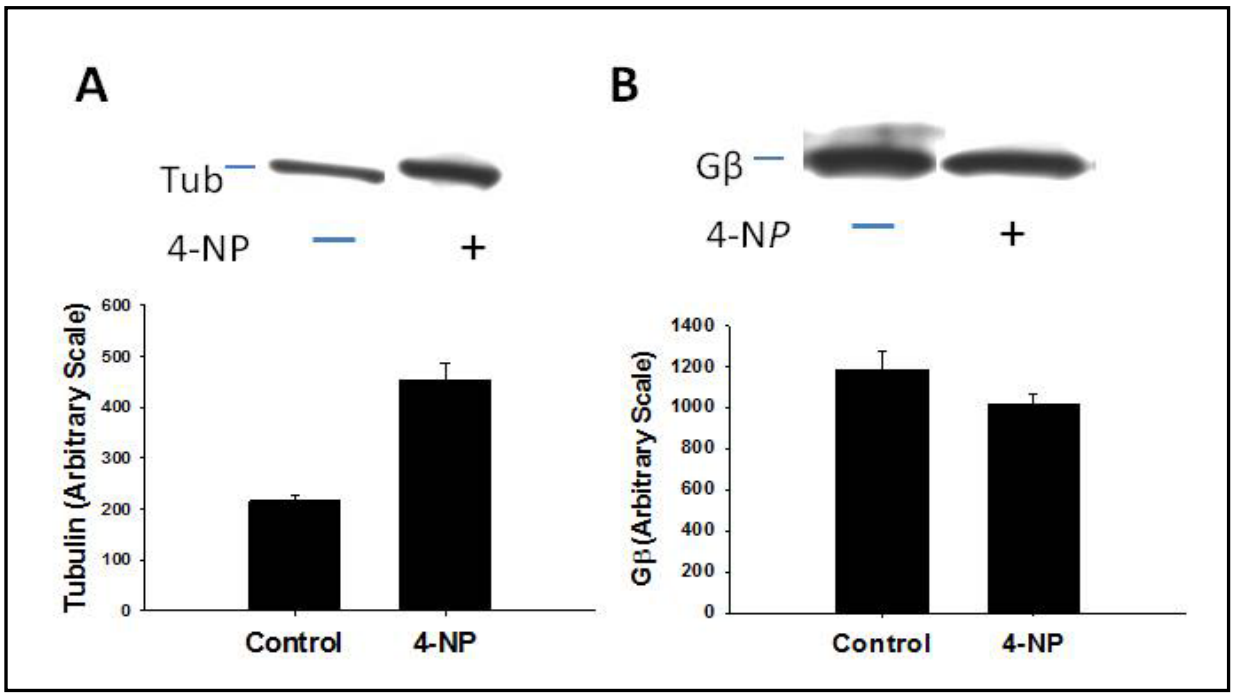

[Figure 11.1 Effect of 4-NP on the expression of Gβγ and Tubulin. PC12 cells were treated with 4-NP at a concentration of 10 μM for 1 hour. After incubation, extraction was performed and whole cell lysate samples were prepared and subjected to Western blot using (A) anti-tubulin antibody or (B) anti-Gβ antibody as indicated in the method. Protein bands were detected using the ECL-plus reagent, quantitated, and expressed**.** Values shown represent mean ± standard error of one experiment done in duplicates]

It is known that tubulin undergoes several post-translational modifications, including tyrosination-detyrosination (addition or removal of tyrosine at the c-terminal end of α-tubulin), and these modifications are important for MT stability. MTs with detyrosinated tubulin (also known as Glu-tubulin) are more stable than MTs comprised of more tyr-tubulin. Because tubulin expression was increased in the presence of 4-NP, we tested whether 4-NP affects the expression

of a specific form of tubulin. As indicated in Figure 11.1, whole-cell lysates were prepared from PC12 cells, treated both in the presence and absence of 4-NP, and subjected to western blotting using anti-tyrosinated tubulin and anti-glutamylated tubulin antibodies. Both tubulin subtypes were affected in the presence of 4-NP (Figure 12.1); however, the effect was more pronounced with glutamylated (Glu-tub) tubulin.

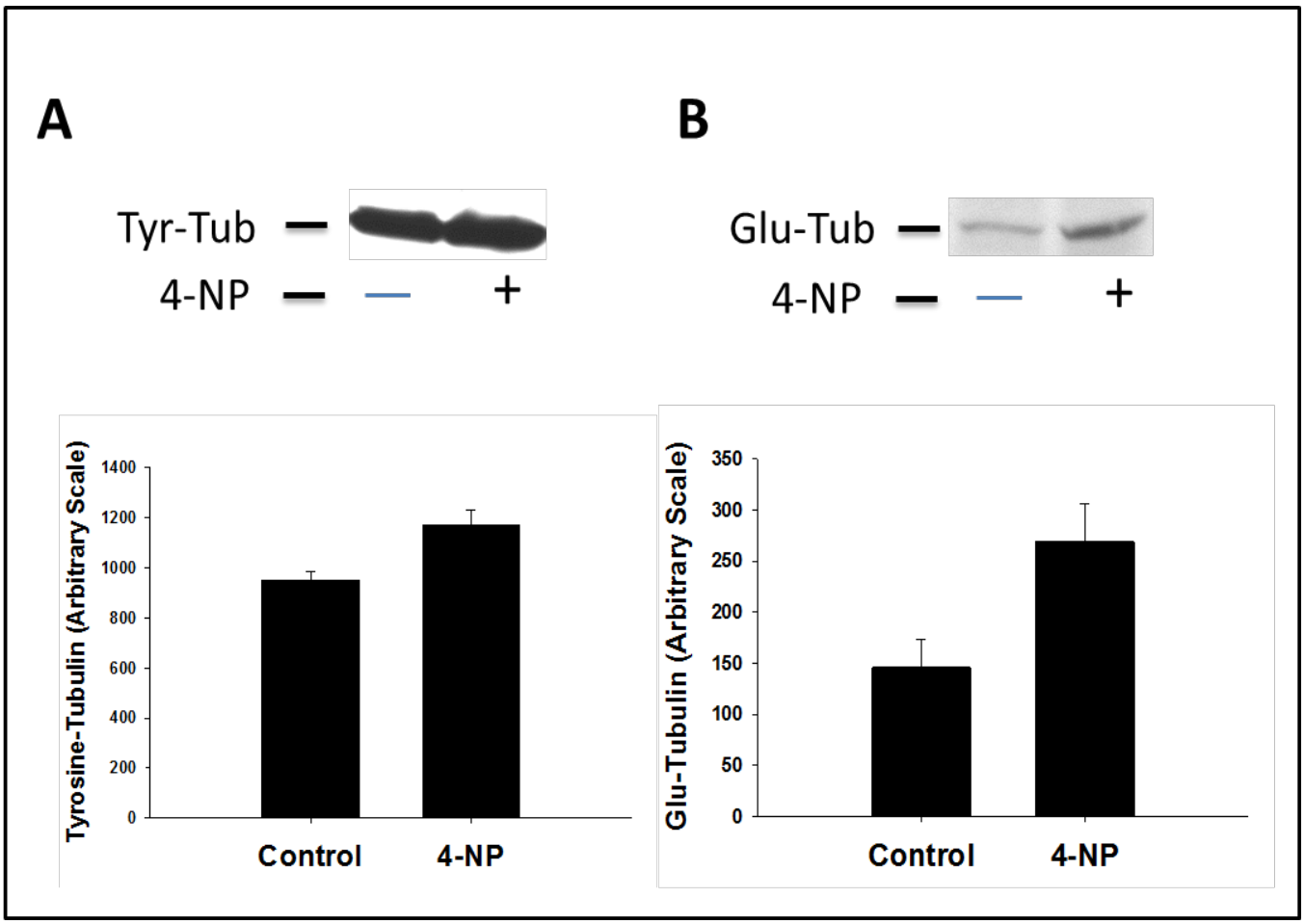

[Figure 12.1 Effect of 4-NP on the expression of Tyrosine and Glutamine Tubulin. PC12 cells were treated with 4-NP at a concentration of 10 μM for 1 hour. After incubation, extraction was performed and whole cell lysate samples were prepared and subjected to Western blot using (A) anti-tyr-tubulin antibody or (B) anti-glu-tubulin antibody as indicated in the method. Protein bands were detected using the ECL-plus reagent, quantitated, and expressed. Values shown represent mean ± standard error of one experiment done in duplicates.]

3.1.6 4-NP does not induce neuronal cell death

To determine if 4-NP induced neuronal cell death at the concentrations used, DNS-cytotoxicity assay was performed as described in the method. This assay uses two fluorescent dyes —Hoechst, which is membrane-permeable and stains the nuclei of both living and dead cells, and propidium iodide (PI), which is only able to enter cells with compromised plasma membranes, thus selectively staining the nuclei of dead cells. PC12 cells were grown on 96 well plates and incubated with NGF and 4-NP at a concentration of 10 μM, followed by 1 h incubation with a mixture of Hoechst/PI at a final concentration of 1 μg/ml. Subsequently, cells were imaged in live mode using a BD Pathway 855 Bioimager system (BD Biosciences) as described in the methods section. The percentage of dead cells in the presence of 4-NP was determined using the BD AttoVision v1.6.2 software (BD Biosciences), and the result was plotted (Figure 12.1B). As indicated in the figure, 4-NP did not cause cytotoxicity on NGF-differentiated PC12 cells and no significant cell death was detected. Hydrogen peroxide (100 μM) was used as a positive control (Figure 12.1A).

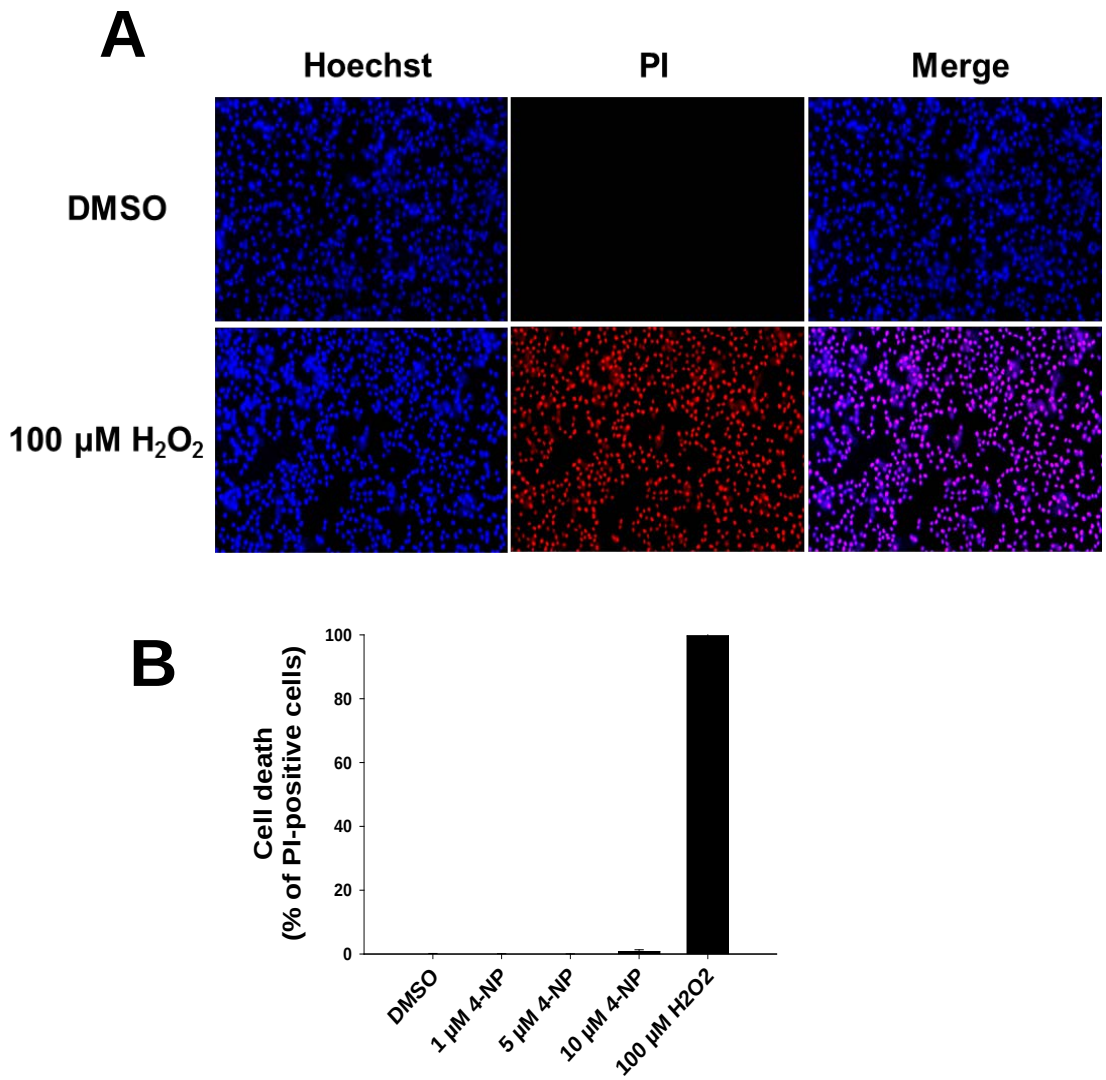

[Figure 13.1 4-NP does not induce neuronal cell death. PC12 cells were grown on 96-well plates and treated with NGF and inhibitors as indicated in Methods. Subsequently, cells were incubated with a Hoechst/propidium iodide (PI) mixture for DNS cytotoxicity assay. The images were captured in live-cell-image mode using confocal automated microscope BD Pathway Bioimager system and a 10x objective, assisted with AttoVision software. **(A)** Representative images corresponding to the same section of 2 x 2 image montages from several conditions (a–l) are shown. H_2O_2 (100 µM) was used as a positive control. Cell nuclei stained with Hoechst provide the total number of cells; cell nuclei stained with PI indicate the number of dead cells; merged Hoechst and PI images, where the magenta color is a consequence of the co-localization of red and blue colors, indicating the number of dead cells in the image. **(B-C)** Cell death was plotted as the percent of PI-positive cells, denoting the total number of dead cells for each condition.]

3.2 Specific Aim-2: Does 4-NP alter cytoskeleton and associated proteins to induce neurodegeneration?

3.2.1 Objective and Overview:

The molecular pathways leading to neurodegeneration are not well understood. As indicated in Figure 2, amyloid plaques and neurofibrillary tangles (NFTs) constitute the two major neuropathologic alterations present in Alzheimer's disease (AD) brains. The majority of past research and drug discovery efforts in the area of neurodegenerative diseases have focused on these pathological markers. Although previous research has advanced our understanding of the pathology of neurodegenerative disorders significantly, the cause of these disorders remains largely unknown. Most importantly, no effective drugs are currently available to treat these neurodegenerative disorders suggesting that there is a critical knowledge gap in our understanding of how the diseases are triggered and progress. Results from Specific Aim-1 indicate that 4-NP inhibits neurite outgrowth from PC12 cells, alters MT and Gβγ organization, and induces cellular aggregation and neurodegeneration. To better understand the role of 4-NP in the disruption of the cytoskeleton and neurodegeneration, in Specific Aim-2, I conducted proteomic analysis of cytoskeletal fractions (CSK) to determine how 4-NP altered the cytoskeleton and associated proteins to induce neurodegeneration. We also attempted biochemical and microscopic analysis to determine whether 4-NP induces aggregation of tau protein while inhibiting neuronal outgrowth and differentiation.

3.2.2 The expression of tau protein increased significantly in the presence of 4-NP

Tau is a microtubule-associated protein found only in axons and it is known to regulate MT assembly and neurite outgrowth. Abnormal phosphorylation of tau is associated with several human neurodegenerative disorders known as taupathies (Alonso et al., 2008; Amniai et al., 2008; Gustav-Rothenberg et al., 2010). In an effort to understand whether 4-NP alters the localization of tau proteins and induces tau aggregation in NGF-differentiated PC12 cells, confocal microscopic analysis was attempted using antibodies specific to tau protein (from Sigma Chemicals). However, two different tau antibodies (monoclonal and polyclonal antibodies) failed to detect tau labeling in NGF-differentiated PC12 cells. Unlike confocal microscopic analysis, tau expression was detected in cell lysates in NGF-differentiated PC12 cells using immunoblot analysis (Figure 14.1). The expression of tau protein is known to increase during neuronal differentiation. It was found that tau expression significantly increased in the presence of 4-NP similar to that observed with tubulin.

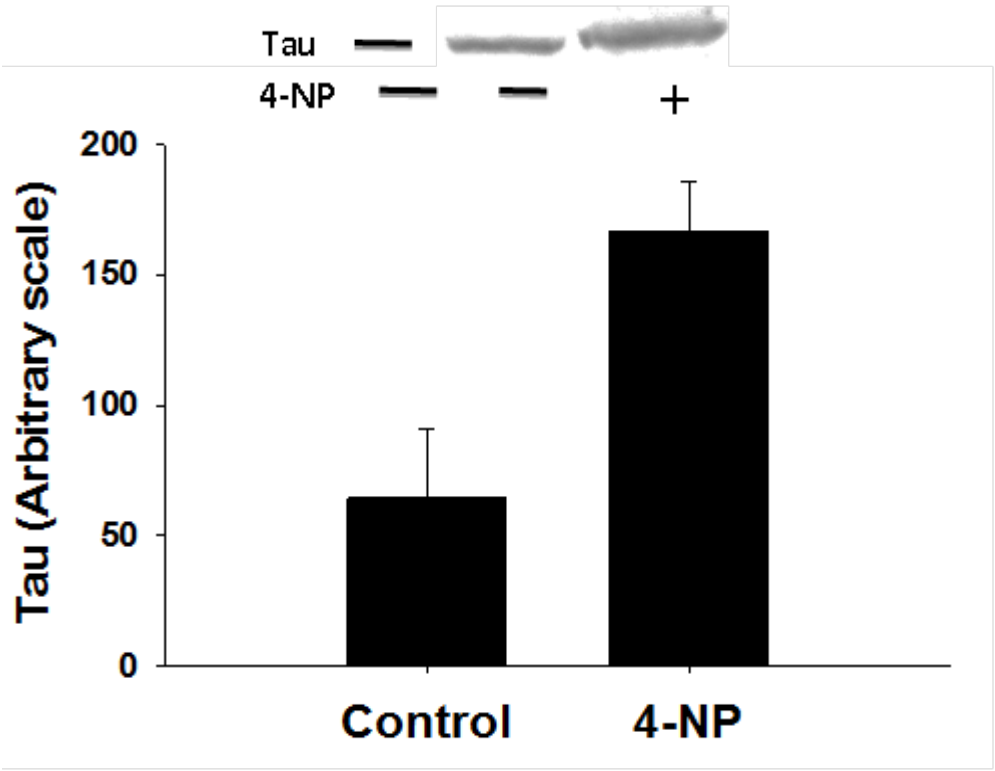

[Figure 141. Effect of 4-NP on the expression of Tau. PC12 cells were treated with 4-NP at a concentration of 10 μM for 1 hour. After incubation, extraction was performed and whole cell lysate samples were prepared and subjected to Western blot using tau antibody as indicated in the method. Protein bands were detected using the ECL-plus reagent, quantitated, and expressed. Values shown represent mean ± standard error of one experiment done in duplicates].

3.2.3 Proteomic analysis of cytoskeletal fraction (CSK)

The cytoskeleton plays a key role in maintaining the highly asymmetrical shape and structural polarity of neurons that are essential for neuronal functions, and is composed of three major protein filaments: actin filaments, microtubules, and intermediate filaments. In addition to several microtubules and actin-associated proteins, motor proteins are also integral components of neuronal cytoskeleton. However, the cytoskeleton is not a static structure. It is highly dynamic in nature with an inherent ability to assemble and disassemble in response to diverse signals. The identity of many of these signaling molecules and how they network spatially within the cell to regulate cytoskeleton remodeling is not well understood and is critical for our understanding of the mechanisms of neurodegeneration. To address this, we carried out proteomic analysis of cytoskeletal fractions both in the presence and the absence of 4-NP. Both control PC12 cells and NGF-differentiated PC12 cells were used for this study.

Proteomic Analysis by mass spectrometry provides a valuable tool to analyze the large numbers of proteins in complex samples and was used for protein analysis of cytoskeletal fraction. Primarily, protein samples were digested with trypsin (residue-specific protease) followed by electrospray ionization directly into the source of a mass spectrometer. Applying a strong electric field performs nebulization of the fluid (containing the sample), and charge peptides by proton attachment. The samples were then delivered to the first mass spectrometer (MS-1), where the peptides are identified based on their mass to charge ratio (*m/z*). The mass spectrometer acquires spectra of the eluting peptides and fragments the most abundant peptide ions in turn. Fragmentation was carried out by collision with an inert gas and occurs mainly at the amide bonds of the peptide, resulting in a set of peptides differing by the mass of one amino acid. The second mass spectrometer (MS-2) analyzes the *m/z* ratios of the resulting peptide

fragments (Liand and Assmann, 2000). The tandem mass spectra (MS/MS) are then searched against protein databases resulting in the identification of a large number of peptides from which a protein list is compiled (Pandey and Mann, 2000).

3.2.4 Proteomic analysis of cytoskeletal fraction reveals the association of G protein subunits with the cytoskeleton in PC12 cells; NGF appears to modulate this association

Cytoskeletal fraction from PC12 cells was subjected to LC-MS/MS analysis in the Orbitrap analyzer as described in the methods. Protein identifications were performed with Proteome Discoverer software. As expected, many cytoskeletal proteins were identified in cytoskeletal fractions of control PC12 and NGF-differentiated PC12 cells. As predicted from previous studies from our laboratory and the current investigation, G protein β-subunits were also identified consistently in CSK both in control and NGF-differentiated PC12 cells. Lists of protein identification with a minimum of two peptides were used. Several proteins of interest—i.e, cytoskeletal proteins including tubulin and heterotrimeric G protein subunits—are listed in Table 1.1 (control PC12 cells) and Table 2.1 (NGF-differentiated PC12 cells). As indicated in the tables, several tubulin isotypes were found in the cytoskeleton fraction with a high score, reflecting the abundance of these isotypes in CSK. Regarding G protein subunits, Gβ2 and Gβ2-like proteins were consistently associated with CSK fractions of both control and NGF-treated PC12 cells (Table 1.1 and 2.1). NGF-induced differentiation of PC12 cells differentially regulated several proteins. Tubulin and G protein subunits, up- or down-regulated by NGF treatment are in Table 3.1. The fold change is computed as the value that maximizes the likelihood function representing differential expression in spectral counts. FDR (false discovery rate) is calculated from the significance statistics. Notable changes were found with G(i) alpha 2, which was up-regulated dramatically (long-fold change 1.7. p value .0035) in the presence of NGF. Conversely, the Gbeta 2-like protein was down-regulated in the presence of NGF. In addition, tubulin beta 5, MAP-1A, was also up-regulated in the presence of 4-NP. It is

anticipated that these data will allow us to better understand the mechanism of NGF-induced neuronal differentiation.

3.2.5 4-NP alters the expression of tubulin isotypes and several cytoskeletal proteins in NGF-differentiated PC12 cells

Proteomic analysis of CSK fraction indicates that 4-NP up-regulates expression of several tubulin isotypes in NGF-differentiated PC12 cells (Table 4.1). This data is interesting and support our western blot results indicating the increased expression of tubulin in the presence of 4-NP in NGF-differentiated cells (Figures 11.1 and 12.1). As indicated in Table 4.1, the tubulin alpha chain-like protein was up-regulated profoundly (about 70 fold) after 4-NP treatment, which suggests a possible role of this tubulin subtype in 4-NP-induced neuronal degeneration. As indicated in Table 4.1, expressions of Gbeta subunits were not affected by 4-NP treatment. However, in addition to tubulin, several cytoskeletal proteins were up- or down-regulated in the presence of 4-NP (Table 4.1). Interestingly, cortactin, an actin-binding protein was down-regulated after 4-NP treatment although it up-regulated significantly in NGF-differentiated cells, suggesting that 4-NP may target this protein to induce neuronal damage. We also carried out proteomic analysis of CSK fraction after treatment with 4-NP in control PC12 cells (without NGF treatment). The data shown in Table 5.1 indicates that tubulin isotypes were not affected in PC12 cells, and the effect of 4-NP was specific in NGF-differentiated PC12 cells. Interestingly, G beta2-like protein and G(i) alpha2 were down-regulated in the presence of 4-NP. We also found tropomyosin alpha-3 chain, and inositol 1,4,5-tryphosphate receptor type-3 was consistently associated with CSK fraction and was up-regulated in 4-NP treated cells.

TABLE 1.1 : Tubulin and heterotrimeric G protein subunits enriched in Cytoskeletal fraction of PC12 cell

Accession No.	PROTEIN ID	Scores	Unique Peptides	Peptide	M.Wt (KDa)
P68370	Tubulin alpha 1A	416.58	1	22	
Q6P9V9	Tubulin alpha 1B	551.47	4	20	
QbAyz1	Tubulin alpha 1C	359.59	2	22	
P85108	Tubulin alpha 2A	656.5	1	20	
Q5XIF6	Tubulin alpha 4A	361.79	4	19	49.9
Q4qRB$	Tubulin beta-3	369.14	2	20	49.6
P69897	Tubulin beta-5	751.02	4	25	50.4
G5ATH6	Guanine Nucleotide binding protein G(I)/G(S)/G(T) subunit beta-1				
P54313	Guanine Nucleotide binding protein G(I)/G(S)/G(T) subunit beta-2	35.49	8	8	37.3
G3V6P8	Guanine Nucleotide binding protein subunit gamma	n.d			
	Guanine Nucleotide binding protein Gi alpha2	n.d			
P63245	Guanine Nucleotide binding beta-2 like	222.49	17	17	35.1
GJBMR4	Guanine Nucleotide binding protein protein G(O) subunit alpha	n.d			
D4A8C9	Guanine Nucleotide binding protein like 3	47.12	8	8	57
	Lamin A				
	Cortactin				
	Tropomyosin alpha-3 chain				
	Inositol 1,4,5- tryphosphate receptor type-3				
	Alpha-actinin-4				
	Actin cytosplasmic-1				
	Peripherin				
P34926	Microtubule-associated protein 1A	5.01	2	2	299.3
P15205	Microtubule-associated protein 1B	8.58	2	2	269.3
G5BF21	Microtubule-associated protein 1A/1B light chain 3B	5.99	2	2	12.9

n.d Not Detected

TABLE 2.1 : Identity of proteins in the Cytoskeletal fraction of NGF-differentiated PC12 cells

Accession No.	PROTEIN ID	Scores	Unique Peptides	Peptide	M.Wt (KDa)
	Tubulin alpha 1A				
Q6P9V9	Tubulin alpha 1B				
	Tubulin alpha 1C	414.37	9	19	
	Tubulin alpha 2A	642.41	2	21	
Q5XIF6	Tubulin alpha 4A	391.93	6	16	49.9
Q4QRB4	Tubulin beta-3	303.8	2	20	49.6
P69897	Tubulin beta-5	786.64	4	25	50.4
	Guanine Nucleotide binding protein G(I)/G(S)/G(T) subunit beta-1				
P54313	Guanine Nucleotide binding protein G(I)/G(S)/G(T) subunit beta-2	34.28	9	9	37.3
G3V6P8	Guanine Nucleotide binding protein subunit gamma	7.80	2	2	8
G5BMR4	Guanine Nucleotide binding protein protein G(O) subunit alpha (Fragmented)	22.88	3	6	
P63245	Guanine Nucleotide binding beta-2 like	144.72	18	18	35.1
Q81159 D4A8C9	Guanine Nucleotide binding protein like 3	71.78	13	13	60.6
	Lamin A				
	Cortactin				
	Tropomyosin alpha-3 chain				
	Inositol 1,4,5- tryphosphate receptor type-3				
	Alpha-actinin-4				
	Actin cytosplasmic-1				
	Peripherin				
P34926	Microtubule-associated protein 1A				
P15205	Microtubule-associated protein 1B				
E9PTL3	MAP	6.53	2	2	52.9
G5BF21	Microtubule-associated protein 1A/1B light chain 3B (Fragment)	3.21	2	2	12.9

TABLE 3.1: Effect of NGF on the upregulation and downregulation of cytoskeletal and GTP-binding proteins in PC12 cells.

PROTEIN	UP-OR DOWN-REGULATED/LOG FOLD CHANGE	FDR
Tubulin alpha 1B	n.c	
Tubulin alpha 1C	n.c	
Tubulin alpha 4A	n.c	
Tubulin beta-3	n.c	
Tubulin beta-5	↑ 0.19	0.037831
Guanine Nucleotide binding beta-1	n.c	
Guanine Nucleotide binding beta-2	n.c	
Guanine Nucleotide binding gamma	n.c	
Guanine Nucleotide binding protein G(i) subunit-alpha2	↑ 1.709	0.0035
Guanine Nucleotide binding beta-2 like	↓-0.401	0.009
Lamin A	↑ 0.245	
Cortactin	↑ 1.134	0.0
Tropomyosin alpha-3 chain	↑0.371	.01
Inositol 1,4,5- tryphosphate receptor type-3	↑ 0.697	0
Alpha-actinin-4	↓ -0.29	0.000868
Microtubule-associated protein 1A	↑1.229	n.s
Microtubule-associated protein 1B	↑ .68	n.s
Microtubule-associated protein	↑ 1.3	n.s

↑ upregulation
↓ downreagulation
n.c. No Change
n.s Not significant
FDR (False Discovery Rate), <.05 significant

TABLE 4.1: Effect of 4-NP on the upregulation and downregulation of cytoskeletal and GTP-binding proteins in NGF-differentiated PC12 cells

PROTEIN	UP-OR DOWN-REGULATED/LOG FOLD CHANGE (+4-NP)	FDR
Tubulin alpha 1C	↑ 0.38	.000001
Tubulin alpha 1B	↑ 0.34	.000023
Tubulin alpha 4A	↑ 0.443	0.0
Tubulin alpha chain-like 3	↑1.968	.000985
Tubulin beta-3	↑ 0.69	0.0
Tubulin beta-5	↑0.377	0.0
Guanine Nucleotide binding protein G(I)/G(S)/G(T) subunit beta-1	n.c	
Guanine Nucleotide binding protein G(I)/G(S)/G(T) subunit beta-2	n.c	
Guanine Nucleotide binding protein subunit gamma	n.c	
Guanine Nucleotide binding protein Gi alpha2	n.c	
Guanine Nucleotide binding beta-2 like	n.c	
Guanine Nucleotide binding protein like 3	n.c	
Guanine Nucleotide binding protein G(O) subunit alpha	n.c	
Cortactin	↓ -.66	0.002308
Alpha actinin-4	n.c	
Actin cytosplasmic-1	n.c	
Peripherin	n.c	
Microtubule-associated protein 1A	n.c	
Microtubule-associated protein 1B	n.c	
Microtubule-associated protein 6	n.c	
Microtubule-associated protein 1	n.c	
Microtubule-associated protein	n.c	

↑ upregulation
↓ downreagulation
n.c. No Change
FDR (False Discovery Rate), <.05 significant

TABLE 5.1 Effect of 4-NP on the upregulation and downregulation of cytoskeletal and GTP-binding proteins in PC12 cells (in absence of NGF).

PROTEIN	UP-OR DOWN-REGULATED (-NGF)	FDR
Tubulin alpha 1C	n.c	
Tubulin alpha 1B	n.c	
Tubulin alpha 4A	n.c	
Tubulin beta-3	n.c	
Tubulin beta-5	n.c	
Guanine Nucleotide binding protein G(I)/G(S)/G(T) subunit beta-1	n.c	
Guanine Nucleotide binding protein G(I)/G(S)/G(T) subunit beta-2	n.c	
Guanine Nucleotide binding protein subunit gamma	-	
Guanine Nucleotide binding beta-2 like 1	↓-0.533	0.0038
Lamin A	n.c	
Cortactin	n.c	
Tropomyosin alpha-3 chain	↑ 0.85	0.003523
Inositol 1,4,5- tryphosphate receptor type-3	n.c	
Alpha-actinin-4	n.c	
Peripherin	↑ .029	0.000293

↑ upregulation
↓ downreagulation
n.c. No Change
FDR (False Discovery Rate), <.05 significant

CHAPTER 4: DISCUSSION

Because the U.S population is growing older, and aging is the most consistent risk factor of developing a neurodegenerative disorder, neurodegenerative diseases are expected to surge in the coming years. Since the pathogenesis of many of these diseases is unknown, the role of environmental factors must be considered. Until recently, the major concerns of environmental factors on human health were centered on potential roles in cancer. However, attention is now focused on understanding the damaging role of environmental factors on developing and mature nervous systems. Recent evidence suggests that environmental chemicals that act as endocrine disruptors (EDC) may adversely affect brain development and induce neurodegeneration. The results presented in this study demonstrate that 4-Nolylphenol (4-NP), an EDC, inhibits NGF-induced neuronal differentiation of PC12 cells by altering MT-Gβγ association. Dynamic rearrangement of microtubules (MTs) is critical for growth-cone motility and neurite outgrowth. Previously, Gβγ has been shown to play a key role in this process by stimulating MT assembly required for neurite outgrowth. This was further supported by the fact that blocking Gβγ-MT interaction by a Gβγ-sequestering peptide, GRK2i, inhibited neurite outgrowth and induced neurodegeneration (Sierra Fonseca et. al., Manuscript in preparation). The observation that 4-NP alters MT organization and its association with Gβγ suggests that 4-NP induces neurodegeneration by affecting the Gβγ-MT mediated pathway.

Proteomic analysis of cytoskeletal fraction (CSK) of 4-NP-treated PC12 cells (both control PC12 and NGF-differentiated cells) produced many interesting results. Because of the insoluble nature of CSK fraction, little attempt was made in the past to carry out proteomic analysis of this cellular structure. However, recently, while this study was in progress, a group of

investigators claimed to enrich CSK fraction from mouse embryonic fibroblasts for proteomic analysis (Choi et.al., 2013; Klemke et. al., 2013). Although this analysis indicated that actin cytoskeleton and focal adhesion-associated proteins were preserved in CSK preparation, microtubule cytoskeleton was disrupted during the purification steps used by these investigators. Our result indicates that (Table 1.1–Table 5.1) MTs and other cytoskeletal proteins were preserved in CSK fraction isolated using our protocol. In addition, heterotrimeric G protein subunits (β, and γ) were found to be associated with cytoskeletal fractions. This finding supports the core hypothesis of our laboratory research—that Gβγ is an integral component of cell cytoskeleton. The result also suggests that NGF-induced neuronal differentiation involves up- or down-regulation of these proteins. Proteomic analysis as well as western blotting reveals that 4-NP up-regulated tubulin expression significantly (Table 4.1, Figure 11.1 and 12.1). The result initially appeared surprising. However, careful analysis of the data and the existing literature I derived a logical explanation of this data. It has been shown earlier that tubulin synthesis in cell is regulated by an autoregulatory mechanism where level of tubulin monomer/dimer guide the synthesis of tubulin mRNA expression in cells (Caron and Kirschner., 1986). Therefore, it is likely that the disruption of MTs observed in the presence of 4-NP altered the tubulin polymer-monomer equilibrium in cells, followed by reduced level of tubulin monomer which subsequently triggered tubulin synthesis. Cartelli et al also observed a significant increase in neuron-specific βIII tubulin and enrichment of detyr-tubulin in dopaminergic neurons in experimental parkinsonium induced by MPTP in C51B1 mice (Cartelli et al., 2013)

Although confocal microscopic analysis indicated that 4-NP disrupted MT organization, biochemical analysis did not show any changes in the level of MT assembly in the presence of 4-NP (Fig.10). The result could be explained by the fact that 4-NP did not cause depolymerization

of MTs, rather induced tubulin aggregation by disrupting MT formation. Since, aggregated proteins remain in the polymeric form, the net change in polymer-monomer equilibrium was not altered by 4-NP.

In summary, I have demonstrated that 4-NP at a concentrations as low as 0.2μM (44.07 μg/L) blocked neurite outgrowth and at higher concentration (5-10μM, ~1000-2000μg/L) induced cellular aggregation and neurodegeneration. Most NP-effect is associated with water concentration ranging from 1 to 1000μg/L (California Environmental Protection Agency, 2009). Concentrations of 4-nonylphenol in surface waters are in the range of 0.11 to 180 micrograms per liter. (Tanghe and Verstraete, 2001). However, this concentration may not reflect 4-NP exposure in the environment, based on 4-NP's low solubility and hydrophobicity, and higher concentrations often detected in Biosolid and sediment samples. Using PC12 cells as a model system, our study clearly demonstrates the potential risk of 4-NP in affecting neuronal development and inducing neurodegeneration, and should provide essential information in accessing environment risk of 4-NP.

REFERENCES

Alonso, A.C., Li, B., Grundke-Iqbal, I., Iqbal, K. 2008. Mechanism of tau-induced neurodegeneration in Alzheimer disease and related tauopathies. Curr. Alzheimer Res. 5, 375-384.

Amniai L, Barbier P, Sillen A, Wieruszeski JM, Peyrot V, Lippens G, and Landrieu I. 2008. Alzheimer disease specific phosphoepitopes of Tau interfere with assembly of tubulin but not binding to microtubules. *FASEB J.* 23, 1146–11452.

Bevan CL, Porter DM, Schumann CR, Bryleva EY, Hendershot TJ, Liu H, Howard MJ, Henderson LP 2006. The endocrine-disrupting compound, nonylphenol, inhibits neurotrophin-dependent neurite outgrowth. Endocrinology. 147, 4192-204.

Bulinski, J. C., and Gundersen, G. G. 1991. Stabilization of post-translational modification of microtubules during cellular morphogenesis. *Bioessays.* 13**,** 285–293

California Environmental Protection Agency. Office of Environmental Health Hazard Assessment. 2009. Toxicological profile for nolylphenol

Caron, J. M. and Kirschner, M. W. 1986. Autoregulation of tubulin synthesis. Bioessays, 5: 211–216.

Cartelli, D., Ronchi, C., Maggioni, M.G., Rodighiero, S., Giavini, E., Cappelletti, G. 2010. Microtubule dysfunction precedes transport impairment and mitochondria damage in MPP+ -induced neurodegeneration. J.Neurochem. 115, 247-258.

Cartelli D, Casagrande F, Busceti CL, Bucci D, Molinaro G, Traficante A, Passarella D, Giavini E, Pezzoli G, Battaglia G, Cappelletti G. 2013. Microtubule alterations occur early in experimental parkinsonism and the microtubule stabilizer epothilone D is neuroprotective. Scientific Reports. 2013, 3:1837.

Cash, A.D., Aliev, G., Siedlak, S.L., Nunomura, A., Fujioka, H.. Zhu, X., Raina, A., Vinters, H.V., Tabaton, M., Johnson, A.B., Paula-Barbosa, M., Avila, J., Jones, P.K., Castellani, R.J., Smith, M.A., Perry, G. 2003. Microtubule reduction in Alzheimer's disease and aging is independent of tau filament formation. Am. J. Pathol. 162, 1623–1627.

Choi S, Kelber J, Jiang X, Strnadel J, Fujimura K, Pasillas M, Coppinger J, Klemke R. 2013. Procedures for the biochemical enrichment and proteomic analysis of the cytoskeletome. Anal Biochem. 22;446C:102-107. doi: http://dx.doi.org/10.1016/j.ab.2013.10.025

Geraldo, S., Gordon-Weeks, P. R. 2009. Cytoskeletal dynamics in growth-cone steering. *J. Cell. Sci.* 122, 3595–3604.

Gustav-Rothenberg, K., Lerner, A., Bonda, D.J., Lee, H.G., Zhu, X., Perry, G., Smith, M.A. 2010. Biomarkers in Alzheimer's disease: past, present and future. Biomark Med. 4, 15–26.

Goto, R., Kubota, T., and Ibuki, Y. 2004. Degradation of nonylphenol polyethoxylates by ultraviolet B irradiation and effects of their products on mammalian cultured cells. Toxicology 202:237-247.

He, J.C., Gomes, I., Nguyen, T., Jayaram, G., Ram, P.T., Devi, L.A., and Iyengar, R. 2005. The G alpha(o/i)-coupled cannabinoid receptor-mediated neurite outgrowth involves Rap regulation of Src and Stat3. J. Biol. Chem. 280, 33426-33434.

Hu, J., Xie, G., and Aizawa, T. 2002. Products of aqueous chlorination of 4-nonylphenol and their estrogenic activity; Environmental Toxicology and Chemistry; 21, 2034-2039

Igarashi, M., Strittmatter, S., Vartanian, T. Fishman, M. C. 1993. Mediation by G Proteins of Signals That Cause Collapse of Growth Cones. *Science.* 259, 77–84.

Kim, J., Korshin, G.V., Velichenko, A. B. 2005. Comparative study of electrochemical degradation and ozonation of nonylphenol; Wat. Res., 39: 2527-2534

Klemke RL, Jiang X, Choi S, Kelber JA.2013. Proteomic and biochemical methods to study the cytoskeletome. Methods Mol Biol. 1046:203-18. doi: 10.1007/978-1-62703-538-5_12.

Kudo C, Wada K, Masuda T, Yonemura T, Shibuya A, Fujimoto Y, et al. 2004. Nonylphenol induces the death of neural stem cells due to activation of the caspase cascade and regulation of the cell cycle. J Neurochemistry 88,1416–23.

Liand, J. and Assmann, S. M. 2000. Mass Spectrometry. An Essential Tool in Proteome Analysis. *Plant Physiology 123 (3) 807-810.*

Lin, L. 2007. Effects of binary mixtures of xenoestrogens on gonadal development and reproduction in zebrafish. University of Saskatchewan, Saskatoon . 3-10

Lotto, B., Upton, L., Price, D. J., Gaspar, P. 1999. Serotonin receptor activation enhances neurite outgrowth of thalamic neurons in rodents. *Neurosci. Lett.* 269, 87–90.

Montoya, V., Gutierrez, C., Najera, O., Leony, D., Varela-Ramirez, A., Popova, J., Rasenick, M. M., Das, S., Roychowdhury, S. 2007. G protein betagamma subunits interact with alphabeta- and gamma-tubulin and play a role in microtubule assembly in PC12 cells. Cell Motil. Cytoskeleton. *64*, 936–950.

Negishi T, Kawasaki K, Suzaki S, et al. 2004. Behavioral alterations in response to fear-provoking stimuli and tranylcypromine induced by perinatal exposure to bisphenol A and nonylphenol in male rats. Environ Health Perspect 112:1159–1164.

Pandey, A. and Mann, M. 2000. Proteomics to study genes and genomes. Nature 405, 837-846

Porter, A. J., and. Hayden, N. J. 2002. Nonylphenol in the Environment: A Critical Review. Department of Civil and Environmental Engineering University of Vermont Burlington, VT 05405.

Reinoso, B. S., Undie, A. S., Levitt, P. 1996. Dopamine receptors mediate differential morphological effects on cerebral cortical neurons in vitro. *J. Neurosci. Res.* 43, 439–453.

Renner, R. (1997) European Bans on Surfactant Trigger Transatlantic Debate. Environ. Sci.Technol. 31, 316A-320A.

Roychowdhury, S., Rasenick, M. M. 1997. G protein beta1gamma2 subunits promote microtubule assembly. *J. Biol. Chem.* 272, 31476–31581.

Roychowdhury, S., Rasenick, M. M. 1997. G protein beta1gamma2 subunits promote microtubule assembly. *J. Biol. Chem.* 272, 31476–31581.

Roychowdhury, S., Panda, D., Wilson, L., Rasenick, M. M. 1999. G protein alpha subunits activate tubulin GTPase and modulate microtubule polymerization dynamics. *J. Biol. Chem.* 13485–13490.

Roychowdhury, S., Martinez, L., Salgado, L., Das, S., and Rasenick, M.M. 2006. G protein activation is prerequisite for functional coupling between Gα/Gβγ and tubulin/microtubules. Biochem. Biophys. Res. Commun. 340, 441-448.

Roychowdhury, S., and Rasenick, M. M. 2008. Submembraneous microtubule cytoskeleton: regulation of microtubule assembly by heterotrimeric G proteins. *FEBS J.* **275,** 4654–4663

Rudel, R.A., Melly, S.J., Geno, P.W., Sun, G. and Brody, J.G. 1998. Identification of Alkylphenols and Other Estrogenic Phenolic Compounds in Wastewater, Septage, and Groundwater on Cape Cod, Massachusetts. Environ. Sci. Technol. 32, 861-869.

Safe, S.H., 2000. Endocrine disruptors and human health--is there a problem? An update. Environmental Health Perspectives 108, 487-493.

Soares, A, Guiegsse, B., Jefferson, B., Cartmell, E., and Lester, J. N. 2008. Nonylphenol in the environment: A critical review on occurrence, fate, toxicity and treatment in wastewaters. Environment International 34, 1033-1049.

Tanghe, T., and Verstraete, W. 2001. Adsorption of nonylphenol onto granular activated carbon; Water, Air, and Soil Pollution; 131:61-72

U.S. Environmental Agency 2010. Overview Nonylphenol (NP) and Nonylphenol Ethoxylates (NPEs) Action Plan [RIN 2070-ZA09].

Witte, H., Bradke, F. 2008. The role of the cytoskeleton during neuronal polarization. *Curr. Opin. Neurobiol.* 18, 479–487.

Jie X., Yang W., Jie Y, Hashim J.H.,Liu X.Y., Fan Q. Y., and Yan L.2010. Toxic effect of gestational exposure to nonylphenol on F1 male rats. Birth Defects Res B Dev Reprod Toxicol. 89(5):418-28. Doi 10.1002/bdrb.20268.

Yoshikawa Y. 2005. Experimental behavioral tests using monkey and rat offspring born from mothers exposed perinatally to EDCs. Psychopharmacol 25:115–124.

CURRICULUM VITA

Jessica Martinez Jurado was born on July 5, 1986 in Chihuahua, Mexico. The first daughter of Rodolfo Martinez and Lourdes Vallejo, she graduated from Monterrey Institute of Technology and Higher Education in Ciudad Juarez, in the spring of 2005 and entered The University of Texas at El Paso in the fall with the Jimmy and Yolanda Janacek scholarship. While pursuing a bachelor's degree in Microbiology, she worked in BURS program. After receiving her bachelor's of science degree from The University of Texas at El Paso in 2010, with the scholarship of Secretaria de Education, Cultura y Deporte of Chihuahua State Government, she entered the Graduate School at The University of Texas at El Paso, where she worked as a teaching assistant for the courses General Biology, Anatomy, and Microbiology.

Permanent Address: 108 Vaquero Lane
El Paso, Texas 79912

This thesis was typed by Jessica Martinez Jurado